

Benign landscapes of low-dimensional relaxations for orthogonal synchronization on general graphs

Andrew D. McRae and Nicolas Boumal*

February 9, 2024

Abstract

Orthogonal group synchronization is the problem of estimating n elements Z_1, \dots, Z_n from the $r \times r$ orthogonal group given some relative measurements $R_{ij} \approx Z_i Z_j^{-1}$. The least-squares formulation is nonconvex. To avoid its local minima, a Shor-type convex relaxation squares the dimension of the optimization problem from $O(n)$ to $O(n^2)$. Alternatively, Burer–Monteiro-type nonconvex relaxations have generic landscape guarantees at dimension $O(n^{3/2})$. For smaller relaxations, the problem structure matters. It has been observed in the robotics literature that, for SLAM problems, it seems sufficient to increase the dimension by a small constant multiple over the original. We partially explain this. This also has implications for Kuramoto oscillators.

Specifically, we minimize the least-squares cost function in terms of estimators Y_1, \dots, Y_n . For $p \geq r$, each Y_i is relaxed to the Stiefel manifold $\text{St}(r, p)$ of $r \times p$ matrices with orthonormal rows. The available measurements implicitly define a (connected) graph G on n vertices. In the noiseless case, we show that, for all connected graphs G , second-order critical points are globally optimal as soon as $p \geq r + 2$. (This implies that Kuramoto oscillators on $\text{St}(r, p)$ synchronize for all $p \geq r + 2$.) This result is the best possible for general graphs; the previous best known result requires $2p \geq 3(r + 1)$. For $p > r + 2$, our result is robust to modest amounts of noise (depending on p and G). Our proof uses a novel randomized choice of tangent direction to prove (near-)optimality of second-order critical points. Finally, we partially extend our noiseless landscape results to the complex case (unitary group); we show that there are no spurious local minima when $2p \geq 3r$.

1 Introduction and results

We examine the optimization landscape of a class of quadratically constrained quadratic programs (QCQPs) that arise from the *orthogonal group synchronization* problem. This widely-studied problem has applications notably in simultaneous localization and mapping (SLAM) [1], cryo-electron microscopy (cryo-EM) [2], computer vision [3], and phase retrieval [4]. It also connects mathematically with oscillator networks [5].

Our main results in this paper are presented in this section as follows: Section 1.1 presents the (real) orthogonal synchronization problem on a graph and our main optimization landscape results for the resulting QCQPs. Section 1.2 connects our work to oscillator networks on (real) Stiefel manifolds and gives a new and optimal result in this field. Section 1.3 partially extends these results to the complex case. Section 1.4 details some specific implications for the low-dimensional groups that are of primary interest in many applications. Section 1.5 gives additional implications of our analysis that may be of independent interest.

*Institute of Mathematics, EPFL, Lausanne (andrew.mcrae@epfl.ch, nicolas.boumal@epfl.ch). This work was supported by the Swiss State Secretariat for Education, Research and Innovation (SERI) under contract number MB22.00027.

1.1 Problem setup and optimization landscape results

The orthogonal synchronization problem we study is the following: Let $G = (V, E)$ be a connected, undirected graph on the vertices $V = \{1, \dots, n\}$ for some integer $n \geq 1$. Each vertex i is associated with an unknown orthogonal matrix $Z_i \in O(r) = \{U \in \mathbf{R}^{r \times r} : UU^\top = I_r\}$. We want to estimate Z_1, \dots, Z_n from (potentially noisy) measurements of the form $R_{ij} = Z_i Z_j^\top + \Delta_{ij} \in \mathbf{R}^{r \times r}$ for each edge $(i, j) \in E$, where Δ_{ij} represents measurement error/noise. Since the measurements are relative, estimation can only be done up to a global orthogonal transformation.

A simple least-squares¹ estimate of Z_1, \dots, Z_n can be obtained from the following optimization problem:

$$\min_{Y \in O(r)^n} \sum_{(i,j) \in E} \|Y_i - R_{ij} Y_j\|_{\mathbb{F}}^2, \quad (1)$$

where $\|\cdot\|_{\mathbb{F}}$ denotes the matrix Frobenius (elementwise ℓ_2) norm. Although the cost function itself is convex in Y , the constraint set $O(r)^n$ is nonconvex. In general, the problem has spurious local minima in which local search methods (such as gradient descent) can get stuck.

Due to the orthogonality constraints, the above problem is equivalent to

$$\max_{Y \in O(r)^n} \sum_{(i,j) \in E} \langle R_{ij}, Y_i Y_j^\top \rangle,$$

where $\langle A, B \rangle = \text{tr}(AB^\top)$ is the Hilbert–Schmidt (or Frobenius) matrix inner product. To write this more compactly, let $C \in \mathbf{R}^{rn \times rn}$ denote the (incomplete) measurement matrix with blocks²

$$C_{ij} = \begin{cases} R_{ij} & \text{if } (i, j) \in E, \\ 0 & \text{otherwise.} \end{cases}$$

With the convention that $R_{ij} = R_{ji}^\top$, the matrix C is symmetric. Then, we can rewrite the problem as

$$\max_{Y \in \mathbf{R}^{rn \times r}} \langle C, YY^\top \rangle \text{ s.t. } Y_i Y_i^\top = I_r, i = 1, \dots, n. \quad (2)$$

The matrix YY^\top is positive semidefinite with rank at most r . Noting that $Y_i Y_i^\top = (YY^\top)_{ii}$, the classical (Shor) convex relaxation consists in replacing YY^\top with a positive semidefinite matrix X , ignoring the rank constraint:

$$\max_{\substack{X \in \mathbf{R}^{rn \times rn} \\ X \succeq 0}} \langle C, X \rangle \text{ s.t. } X_{ii} = I_r, i = 1, \dots, n. \quad (3)$$

This allows the rank of X to grow up to rn . Alternatively, we can allow Y to have $p \geq r$ columns in (2). This effectively allows YY^\top to have rank up to p , providing a more gradual relaxation as we increase p . This yields the rank- p Burer–Monteiro relaxation:

$$\max_{Y \in \mathbf{R}^{rn \times p}} \langle C, YY^\top \rangle \text{ s.t. } Y_i Y_i^\top = I_r, i = 1, \dots, n. \quad (4)$$

We can view the rank $p \geq r$ as a hyperparameter that interpolates the original nonconvex problem (2) (in the case $p = r$) and the full SDP relaxation (3) (which corresponds to $p \geq rn$).

This paper primarily considers the *optimization landscape* of the rank-relaxed nonconvex problem (4) for various values of p . In particular, we ask:

¹More generally, we could consider *weighted* least-squares (e.g., if the noise variance changes across measurements). This corresponds to a graph G with (positively) weighted edges. Our analysis easily extends to this case, but we omit the generalization for simplicity.

²Throughout this paper, indices into a matrix dimension of length rn refer to blocks of r rows or columns. Thus, for $C \in \mathbf{R}^{rn \times rn}$, C_{ij} refers to the (i, j) th $r \times r$ block; for $Y \in \mathbf{R}^{rn \times p}$, Y_i refers to the i th $r \times p$ block of Y , etc.

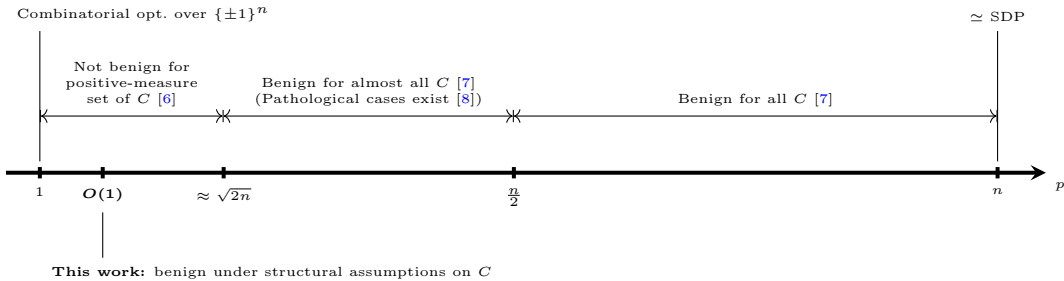


Figure 1: For low-dimensional relaxations, structural assumptions on the data (i.e., the cost matrix C) are necessary for benign nonconvexity. This diagram summarizes known results about the landscape of (4) in the case $r = 1$, that is, relaxation at rank p for synchronization of n elements in $O(1) = \{\pm 1\}$.

Q: *How large does p need to be so (4) has no spurious local optima?*

Much is known (see Figure 1 for a summary in the case $r = 1$): For general cost matrices C , we need³ $p = O(n)$ to guarantee such a benign landscape (resulting in $O(n^2)$ variables, which is the same order as the full SDP relaxation); with the assumption that C is “generic” (outside of a zero measure set), we can reduce this to $p = O(n^{1/2})$ (resulting in $O(n^{3/2})$ variables); for lower values of p , however, “bad” matrices C are plenty: benign landscapes *require* a structured C .

Remarkably, for cost matrices C arising in specific applications, it has been observed that p can be taken much smaller—just slightly above r . This was observed and partially explained theoretically for models related to ours (complete-graph synchronization and stochastic block models) in prior works such as [9, 10]. In the case of synchronization on a general graph for SLAM (robotics), similar empirical observations were reported in [11, 12]; this is the inspiration for our work.

We prove that benign nonconvexity occurs for small values of p for cost matrices C arising from the general-graph synchronization problem; this gives additional theoretical support to the algorithms and empirical observations of [11, 12]. Setting $p = O(1)$ results in an optimization problem with $O(n)$ variables, similar to the original problem (2) but tractable despite being nonconvex.

Specifically, we give conditions under which every *second-order critical point* (in particular, every local optimum) of (4) is a global optimum. We define such a point more precisely in Section 3, but it is, essentially, a point $Y \in \mathbf{R}^{rn \times p}$ where, subject to the constraints, the gradient at Y is zero and all eigenvalues of the Hessian are nonpositive.

We first consider the case with no measurement error (i.e., $R_{ij} = Z_i Z_j^\top$). Clearly, a globally optimal solution to the original least-squares problem (1) is

$$Z := \begin{bmatrix} Z_1 \\ \vdots \\ Z_n \end{bmatrix} \in \mathbf{R}^{rn \times r}.$$

Absent noise, the computational task is trivial: fix $Z_1 = I_r$ arbitrarily (since recovery is up to global orthogonal transformation), then traverse any spanning tree of G , recursively applying the measured relative differences to infer the other Z_i . However, in general, the *landscapes* of (1), (2) have spurious local optima. What is the effect of relaxation then?

Our first main result states that, without noise, relaxing to $p = r + 2$ eliminates spurious optima.

Theorem 1. *Suppose G is connected. If the measurements are exact, i.e., $R_{ij} = Z_i Z_j^\top$ for all $(i, j) \in E$, then, if $p \geq r + 2$, any second-order critical point Y of (4) satisfies $Y Y^\top = Z Z^\top$. Equivalently, $Y = Z U$ for some $r \times p$ matrix U satisfying $U U^\top = I_r$.*

³Big-oh notation $O(\cdot)$ is with respect to n , treating r as a small constant.

This result is tight. Indeed, at $p = r$ and $p = r + 1$, there exist spurious local optima for certain connected graphs G ; see Section 1.2 for further details and discussion.

We next consider the effect of measurement error (noise). Our results do not apply to arbitrary noise (otherwise they would apply to arbitrary C) but depend on the noise level relative to the graph connectivity.

To quantify the noise, denote by Δ the $rn \times rn$ matrix with the errors Δ_{ij} in the appropriate places for $(i, j) \in E$, setting $\Delta_{ij} = 0$ for $(i, j) \notin E$. Thus, Δ is the portion of the cost matrix C that is due to measurement error. Our results are stated in terms of $\|\Delta\|_{\ell_2}$ (where $\|\cdot\|_{\ell_2}$ denotes matrix operator norm).

We quantify the connectivity of G in a spectral sense. Let $L = L(G)$ be the unnormalized graph Laplacian of G , defined as $L = \text{diag}(A\mathbf{1}) - A$, where A is the adjacency matrix of G and $\mathbf{1} \in \mathbf{R}^n$ is the all-ones vector. The matrix L is positive semidefinite with eigenvalues $0 = \lambda_1 \leq \lambda_2 \leq \dots \leq \lambda_n = \|L\|_{\ell_2}$. If G is connected, $\lambda_2 > 0$. The better G is connected, the larger λ_2 is; λ_2 is often called the *algebraic connectivity* or *Fiedler value* of G .

With these definitions in place, we can state our first noisy landscape result:

Theorem 2. *Suppose G is connected and $p > r + 2$. Define*

$$C_p := \frac{2(p + r - 2)}{p - r - 2}.$$

Then any second-order critical point Y of (4) satisfies

$$\text{rank}(Y) \leq r + 5C_p^2 \left(\frac{\|\Delta\|_{\ell_2}}{\lambda_2} \right)^2 rn.$$

If, furthermore, $p > r + 5C_p^2 \left(\frac{\|\Delta\|_{\ell_2}}{\lambda_2} \right)^2 rn$, then Y is a globally optimal solution to (4), and YY^\top is an optimal solution to the SDP (3).

This result quantitatively bounds how large p needs to be so that (4) has a benign landscape and yields an exact solution to the full SDP relaxation. The bound depends on the effective signal-to-noise ratio $\|\Delta\|_{\ell_2}/\lambda_2$.

When Theorem 2 ensures that $\text{rank}(Y) = r$ exactly, we obtain a stronger result:

Theorem 3. *Suppose G is connected and $p > r + 2$. Let C_p be as defined in Theorem 2. If*

$$\|\Delta\|_{\ell_2} < \frac{\lambda_2}{\sqrt{5}C_p\sqrt{rn}}, \tag{5}$$

then any second-order critical point Y of (4) satisfies the following:

- Y is the unique solution to (4) up to a global orthogonal transformation.
- Y has rank r and hence can be factored as $Y = \widehat{Z}U$ for some $\widehat{Z} \in \mathbf{R}^{rn \times r}$ and $U \in \mathbf{R}^{r \times p}$ such that $UU^\top = I_r$. Moreover, \widehat{Z} is the unique solution of (2) up to a global orthogonal transformation.
- YY^\top is the unique solution to the SDP (3).

First, note that if the measurement error Δ is small enough, then $p = r + 3$ suffices to obtain a benign landscape. This provides baseline robustness for Theorem 1.⁴ Furthermore, the second-order critical points yield a global solution to the original, unrelaxed problem (2), which does not (in general) have a benign landscape.

⁴The noiseless result Theorem 1 is already robust to noise when $p = r + 2$, but the required bound on $\|\Delta\|_{\ell_2}$ might be much worse. See Section 4.2 for details.

If the measurement graph G is complete, $\lambda_2 = n$, so the condition (5) becomes⁵ $\|\Delta\|_{\ell_2} \lesssim_{p,r} \sqrt{n}$. If the elements of Δ are, for example, i.i.d. Gaussian with variance σ^2 , this requires $\sigma^2 \lesssim_{p,r} 1$. More generally, if G is an Erdős–Rényi graph with edge probability q , and $q \gtrsim \frac{\log n}{n}$ (which is necessary for G to be connected), we will have, with high probability, $\lambda_2 \approx nq$ (see [13]). In the i.i.d. Gaussian noise case, we have, with high probability, $\|\Delta\|_{\ell_2} \approx \sigma\sqrt{nq}$ (see, e.g., [14]), so the condition on the noise variance becomes $\sigma^2 \lesssim_{p,r} q$.

In some cases, the assumptions of Theorems 2 and 3 appear to be stronger than necessary (i.e., too pessimistic). Our numerical experiments in Section 6 strongly suggest this for i.i.d. Gaussian noise. It is also pessimistic compared to existing theoretical results for the complete-graph case. Existing theory (e.g., [10]—see Section 2.1 for more references), under an additional assumption that the rows of Δ are not too correlated with Z , only requires $\|\Delta\|_{\ell_2} \lesssim n^{3/4}$. However, the techniques used are specialized to the complete-graph case, and it is not clear how to adapt our methods in a way that recovers the best existing results when G is the complete graph (see the end of Section 4.3.2). Furthermore, it is unclear whether our requirements in Theorems 2 and 3 are still too pessimistic in the general adversarial-noise case.

1.2 Implications for oscillator network synchronization

Another way to view the problem we have just described is *oscillator synchronization*. We briefly describe this connection here and spell out a corollary from Theorem 1. See, for example, [15, 5] for more detailed discussion and derivations.

Given a connected graph⁶ G defined as before, a simple version of the *Kuramoto* model for an oscillator network on G is the following: we have time-varying angles $\theta_1(t), \dots, \theta_n(t)$ associated with the n vertices, and these angles follow

$$\dot{\theta}_i = - \sum_{j \in \mathcal{N}_i} \sin(\theta_i - \theta_j), \quad i = 1, \dots, n, \quad (6)$$

where \mathcal{N}_i is the set of neighbors of vertex i in G . One can easily check that these dynamics are the gradient flow for the following optimization problem:

$$\max_{\theta \in \mathbf{R}^n} \frac{1}{2} \sum_{i,j=1}^n A_{ij} \cos(\theta_i - \theta_j). \quad (7)$$

Clearly, the optima of (7) are the “synchronized” states $\theta_1 = \dots = \theta_n \pmod{2\pi}$. Many papers have studied this model, particularly with the following question in mind:

Q: *For which graphs G does the dynamical system (6) converge to a synchronized state as $t \rightarrow \infty$ for “generic” initial conditions?*

Generic means “except for a zero-measure set” so that this happens with probability 1 if $\theta_1(0), \dots, \theta_n(0)$ are chosen uniformly at random over $[0, 2\pi)$.

To connect this problem to our work, note that (7) is a reparametrization of the problem (4) in the case $r = 1, p = 2$ when $Z_i = 1$ for all i and the measurements are exact.⁷ There are many examples (see, e.g., [17]) of connected graphs G under which (7) has spurious local optima with strictly⁸ negative definite Hessian (and to which, therefore, gradient flow will converge if initialized in some positive-measure neighborhood). This implies that (4) *does not* always have a benign landscape

⁵Here and throughout the paper, $a \lesssim b$ ($a \gtrsim b$) means $a \leq cb$ ($a \geq cb$) for some unspecified constant $c > 0$. With subscripts, $a \lesssim_{p,r} b$ means $a \leq c(p,r)b$ (i.e., the “constant” could depend on r and p).

⁶Again, the problem and our analysis easily extend to (positively) weighted edges.

⁷Explicitly, $\theta_i \mapsto Y_i = [\cos(\theta_i), \sin(\theta_i)]$ so that $\cos(\theta_i - \theta_j) = Y_i Y_j^\top$. In this case, the cost matrix C is equal to the adjacency matrix A of G . The differential of the change of variable is surjective, hence it does not introduce spurious critical points [16, Proposition 9.6]; thus the landscapes in θ and in Y are qualitatively the same.

⁸Modulo the trivial direction that shifts all angles equally.

for $r = 1, p = 2$. However, this changes when one studies the “synchronization” landscape for higher-dimensional “oscillators.”

For $r \geq 1$, consider (4) in the case that $Z_1 = \dots = Z_n = I_r$.⁹ Furthermore, assume that there is no measurement error,¹⁰ so $R_{ij} = Z_i Z_j^\top = I_r$ for all $(i, j) \in E$. Note, furthermore, that the feasible points $Y = [Y_i]_i$ lie in a product of *Stiefel manifolds* (we develop this connection further in the proofs of our main results):

$$\text{St}(r, p) = \{U \in \mathbf{R}^{r \times p} : UU^\top = I_r\}.$$

With these simplifications and notation, problem (4) becomes (within a factor of 2)

$$\max_{Y \in \text{St}(r, p)^n} \frac{1}{2} \sum_{i, j=1}^n A_{ij} \text{tr}(Y_i Y_j^\top), \quad (8)$$

where A is the adjacency matrix of G . Again, the global optima are precisely the Y such that $Y_1 = \dots = Y_n \in \text{St}(r, p)$.

Any trajectory $Y(t)$ of the gradient flow on the constraint manifold satisfies the following system of differential equations:

$$\dot{Y}_i = -\mathcal{P}_{T_{Y_i}} \left(\sum_{j \in \mathcal{N}_i} (Y_i - Y_j) \right), \quad i = 1, \dots, n. \quad (9)$$

Here, T_U denotes the tangent space of $\text{St}(r, p)$ at U (see Section 4), and \mathcal{P}_{T_U} is the (Euclidean) orthogonal projection onto T_U . These dynamics are (a simple version of) the Kuramoto model for a network of Stiefel-manifold valued oscillators.

Once again, we ask the question: when does the Stiefel-manifold valued Kuramoto oscillator network governed by (9) *synchronize* (i.e., converge to a synchronized state $Y_1 = \dots = Y_n$ as $t \rightarrow \infty$ for generic initialization)? The remarkable results of [18, 15, 5] show that for certain manifolds, Kuramoto oscillator networks synchronize for *any* connected graph G . Specifically, the paper [18] shows that for all $p \geq 3$, oscillator networks on $\text{St}(1, p)$ (equivalently on the d -sphere S^d for $d \geq 2$) always synchronize for connected G . This was extended in [15, 5] to show that $\text{St}(r, p)$ oscillator networks synchronize if $2p \geq 3(r + 1)$.

In this paper, we prove that $\text{St}(r, p)$ -valued oscillator networks synchronize under the weaker condition $p \geq r + 2$. This is a simple corollary of the noiseless orthogonal group synchronization result, Theorem 1.

Corollary 1. *For any connected graph G , the $\text{St}(r, p)$ -valued Kuramoto oscillator network on G synchronizes if $p \geq r + 2$.*

This result is tight and thus positively solves a conjecture in [5, 19]. More precisely, we have shown that general connected oscillator networks on $\text{St}(r, p)$ synchronize if and only if the manifold is *simply connected* (this is equivalent to $p \geq r + 2$: see, e.g., [20, Example 4.53]). If the manifold is not simply connected, one can easily construct graphs G such that (9) has a stable equilibrium other than the synchronized state [21].

Corollary 1 follows from Theorem 1 by the same arguments used to prove [22, Theorem 5.1]. Theorem 1 implies that any critical point that is not the fully synchronized state is a strict saddle point of (8) (i.e., the Riemannian Hessian has at least one strictly positive eigenvalue). Because $\text{St}(r, p)^n$ is compact, each gradient flow trajectory has at least one limit point (and any limit point is a critical point). As $\text{St}(r, p)^n$ and the objective function are real analytic, each trajectory must in fact converge to a single critical point ([23], [24, p. 4]). By [22, Lemma B.1], the set of $Y(0)$ for which $Y(t)$ converges to a strict saddle has zero measure. Then, for all $Y(0)$ outside this zero-measure set, $Y(t)$ must converge to a fully-synchronized state.

⁹This is without loss of generality as we can always smoothly change variables to bring the ground truth to this position without affecting the landscape: see Section 4 for details.

¹⁰The simple connection to oscillators outlined here is most meaningful in the noiseless case.

1.3 The complex case

We can extend the previous (real) orthogonal matrix estimation problem to the complex case. Here, we seek to estimate *unitary* matrices $Z_1, \dots, Z_n \in \mathbf{U}(r) := \{U \in \mathbf{C}^{r \times r} : UU^* = I_r\}$ given measurements of the form $R_{ij} \approx Z_i Z_j^*$. We form our cost matrix $C \in \mathbf{C}^{rn \times rn}$ (C is now *Hermitian*, i.e., $C = C^*$) and consider the relationships between the original unitary group least-squares problem

$$\max_{Y \in \mathbf{C}^{rn \times r}} \langle C, YY^* \rangle \text{ s.t. } Y_i Y_i^* = I_r, i = 1, \dots, n, \quad (10)$$

the SDP relaxation

$$\max_{\substack{X \in \mathbf{C}^{rn \times rn} \\ X \succeq 0}} \langle C, X \rangle \text{ s.t. } X_{ii} = I_r, i = 1, \dots, n, \quad (11)$$

and the rank- p relaxation

$$\max_{Y \in \mathbf{C}^{rn \times p}} \langle C, YY^* \rangle \text{ s.t. } Y_i Y_i^* = I_r, i = 1, \dots, n. \quad (12)$$

We denote the complex $r \times p$ Stiefel manifold by

$$\text{St}(r, p, \mathbf{C}) = \{U \in \mathbf{C}^{r \times p} : UU^* = I_r\}.$$

For simplicity, we only consider the noiseless landscape. Again, the result has implications for Kuramoto oscillators on the complex Stiefel manifold, which are related to the “quantum Kuramoto model” on unitary matrices ([25]; see Section 2.3 for additional references).

Theorem 4. *Suppose G is connected, and the measurements are exact (i.e., $R_{ij} = Z_i Z_j^*$ for $(i, j) \in E$). If $2p \geq 3r$, then any second-order critical point Y of (12) satisfies $YY^* = ZZ^*$. Consequently, the $\text{St}(r, p, \mathbf{C})$ -valued Kuramoto oscillator network on G synchronizes.*

Due to the $3/2$ factor and certain similarities in the proof, this can also be seen as a complex adaptation of the result in [5]. Curiously, the innovations that allow us to improve that previous result in the real case do not easily carry over to the complex case; see the proof in Section 5 for further details.

As discussed in Section 1.2, our results for the real case show that we obtain a benign landscape (and all connected oscillator networks synchronize) as soon as the real Stiefel manifold $\text{St}(r, p)$ is *simply connected*. In the complex case, the Stiefel manifold $\text{St}(r, p, \mathbf{C})$ is simply connected as soon as $p \geq r + 1$ (again, see [20, Example 4.53]). We conjecture that this is the correct condition and that therefore Theorem 4 is suboptimal. However, we have been unable to prove this, and it is unclear how to test it empirically.¹¹ If our conjecture is true, it is not clear where the limitations are in our current proof. The critical step in our and others’ proofs is to make an (educated) guess of potential descent direction for the objective function; how to improve this guess is unclear.

1.4 Discussion of small- r synchronization conditions

It is interesting to consider the implications of the noiseless landscape results Theorems 1 and 4 and Corollary 1 for small values of the matrix dimension r , as this covers many applications. See Table 1 for a summary.

¹¹The standard counterexamples to benign landscape/synchronization results are cycle graphs (indeed, the paper [21] uses cycle graphs to show that networks of oscillators taking values in a non-simply-connected manifold do not synchronize in general). We do not expect this counterexample to work in the complex case when $p \geq r + 1$, because a cycle graph corresponds geometrically to the unit circle, that is, $\mathbf{U}(1)$, and our result shows that, if $r = 1$, $p \geq 2 = r + 1$ suffices in the complex case. It is not clear how to construct a higher-dimensional equivalent as a candidate counterexample to our conjecture. For example, intuition from homotopy theory would suggest that we try a graph corresponding geometrically to a higher-dimensional sphere.

Group	Field	r	Min. p req.	Orig. dim.	Min. Stiefel dim.
$O(1) = \mathbf{Z}_2$	\mathbf{R}	1	3	0	2
$U(1) = S^1 = SO(2)$	\mathbf{C}	1	2	1	3
$O(2)$	\mathbf{R}	2	4	1	5
$U(2)$	\mathbf{C}	2	3	4	8
$O(3)$	\mathbf{R}	3	5	3	9
$U(3)$	\mathbf{C}	3	5 (4*)	9	21 (15*)

Table 1: Properties of the groups $O(r)$ and $U(r)$ for $r \leq 3$ and the relaxations required to guarantee synchronization. In the last row, * indicates the result of the conjectured $p \geq r + 1$ condition for the complex case.

For synchronization of *rotations* (rather than orthogonal transformations) in the plane \mathbf{R}^2 , we can adopt two perspectives. We could view $SO(2)$ as one of the two connected components of $O(2)$, in which case Theorem 1 allows us to relax to synchronization on $St(4, 2)$ (a 5-dimensional manifold). Alternatively, we can view $SO(2)$ as isomorphic to $U(1)$ (a circle, S^1), in which case Theorem 4 allows us to relax to synchronization on the *complex* Stiefel manifold $St(2, 1, \mathbf{C})$, which is isomorphic to S^3 (a 3-dimensional sphere).

We have a similar situation for synchronization of rotations in \mathbf{R}^3 . Viewing $SO(3)$ as a subgroup of $O(3)$, we can relax the synchronization to $St(5, 3)$, which is a 9-dimensional manifold. Alternatively, it is well known that we can embed¹² $SO(3)$ in the special unitary group $SU(2)$, which is the subgroup of $U(2)$ of matrices with determinant 1. With this formulation, we can synchronize in $U(2)$ by relaxing to $St(3, 2, \mathbf{C})$, which is an 8-dimensional manifold.

1.5 Additional results

Our analysis yields several additional results of independent interest. For the nonconvex relaxation (4), we show second-order critical points can be good approximate solutions even if they are not globally optimal. For the SDP relaxation (3), we show a tightness result (rank recovery) and an approximation result.

1.5.1 Error bounds for all second-order critical points

Regardless of whether the conditions of Theorems 2 and 3 are satisfied, we can obtain useful error bounds for all second-order critical points Y of (4). Recall that $\|\cdot\|_{\ell_2}$, $\|\cdot\|_F$ respectively denote the operator and Frobenius matrix norms. The quality metric we use for a candidate solution Y is the correlation $\langle ZZ^\top, YY^\top \rangle = \|Z^\top Y\|_F^2$. The maximum value this can take is $n^2 r$ (because $\|ZZ^\top\|_{\ell_2} = n$, and $\text{tr}(YY^\top) = rn$), and this value is reached if and only if $YY^\top = ZZ^\top$ (as in Theorem 1).

Theorem 5. *Assume G is connected and $p > r + 2$. Then any second-order critical point Y of (4) satisfies*

$$\langle ZZ^\top, YY^\top \rangle \geq \left[1 - C_p^2 \frac{\|\Delta\|_{\ell_2}^2}{\lambda_2^2} \right] n^2 r,$$

where C_p is defined in the statement of Theorem 2.

Comparable error bounds have been shown for the eigenvector method; in particular, our bound is identical (within constants and dependence on p) to one in [26]. See Section 2.2 for further references.

¹²More precisely, there is a double covering group homomorphism from $SU(2)$ to $SO(3)$.

In the Erdős–Rényi graph case with i.i.d. zero-mean random noise (see discussion after Theorem 3), we obtain, with high probability,

$$1 - \frac{\langle ZZ^\top, YY^\top \rangle}{n^2 r} \lesssim \frac{\sigma^2}{qn},$$

where q is the edge probability and σ^2 is the noise variance. This is the minimax-optimal error rate for this problem, as shown in [27] (within constants and dependence on r —the error metric in [27] is slightly different and depends differently on r). Again, see Section 2.2 for more references.

1.5.2 Consequences for the SDP relaxation

For the SDP relaxation (3), we first have an exactness result (tight relaxation, rank recovery):

Corollary 2. *Assume G is connected. If $\|\Delta\|_{\ell_2} < \frac{\lambda_2}{2\sqrt{5}\sqrt{rn}}$, then*

- *The SDP relaxation (3) has a unique solution \hat{X} , and $\text{rank}(\hat{X}) = r$.*
- *The unrelaxed problem (2) has a unique (up to orthogonal transformation) solution $\hat{Z} \in \mathbf{R}^{rn \times r}$.*
- *$\hat{X} = \hat{Z}\hat{Z}^\top$.*

Next, we have a general error bound for the SDP relaxation that applies even if the exactness result above does not:

Corollary 3. *Assume G is connected. Any solution X to (3) satisfies*

$$\langle X, ZZ^\top \rangle \geq \left(1 - \frac{4\|\Delta\|_{\ell_2}^2}{\lambda_2^2}\right)n^2 r.$$

These corollaries follow from Theorems 3 and 5 in the limit $p \rightarrow \infty$. To be precise, let X be an optimal solution to (3). For any $p \geq rn$, there exists $Y \in \mathbf{R}^{rn \times p}$ such that $X = YY^\top$. The fact that X is feasible implies that Y is feasible for (4). Furthermore, the optimality of X implies that Y is a global optimum and therefore is a second-order critical point [7, Prop. 2.4]. We then apply Theorems 3 and 5 and take $p \rightarrow \infty$, noting that $C_p \rightarrow 2$. See the discussion in Sections 1.5.1 and 2.2 for comparison to existing error bounds.

2 Related work

The literature on orthogonal group synchronization is vast, appearing in multiple communities such as robotics, image processing, signal processing, and dynamical systems. We highlight a few salient references here; see also [28, 29] for partial surveys. Many of the tools we use in our analysis have been used before. We point this out in our analysis along the way.

2.1 Rank relaxation for synchronization

Low-rank factorizations of SDPs (which, in our case, correspond to partial rank relaxations of the synchronization problem) have a long history. This approach is often called Burer–Monteiro factorization after the pioneering work of those authors (e.g., [30, 31]).

The report [32], along with the more general results in [7], provides a theoretical framework for analyzing Burer–Monteiro factorizations (like ours) of SDPs with (block-)diagonal constraints. The papers [11] and [12] develop fast algorithms (generalized to the special Euclidean group case in [11]), showing that the “Riemannian staircase” approach (iteratively increasing the relaxation rank) proposed in [32] provides an exact solution to the SDP relaxation, but they do not specify what relaxation rank (p in our notation) suffices. Our results provide an upper bound (optimal in the

noiseless case) on how much such algorithms must relax the rank constraint for the synchronization problem.

As far as we are aware, *landscape* results similar to ours have previously only been proved in the complete measurement graph case. For this case, the papers [9, 10] provide error bounds and benign landscape results for rank-relaxed optimization like (4) (for the case $r = 1, p = 2$ in [9]).

The paper [10] analyzes the landscape of (4) in the same general $O(r)$ case that we do and is thus the most comparable work to ours. We can directly compare our Theorem 3 with [10, Theorem 3]. In the complete-graph case, $\lambda_2 = n - 1$, so the condition (5) of Theorem 3 becomes $\|\Delta\|_{\ell_2} \lesssim_{p,r} \sqrt{n}$. This prior result [10, Theorem 3], in the adversarial-noise case (i.e., only assuming a bound on $\|\Delta\|_{\ell_2}$), has a comparable requirement. With additional assumptions on Δ , the prior result improves this to $\|\Delta\|_{\ell_2} \lesssim n^{3/4}$, but the techniques used do not easily carry over to our general-graph case. In addition, the paper [10] requires $p > 2r$ for all its results.

To the best of our knowledge, the partial benign landscape result of Theorem 2 (which gives conditions under which (4) has a benign landscape and yields an exact solution to the SDP even when the solution is not necessarily rank- r) is new even in the complete-graph case.

In a different vein, [33] provides a general bound on how well rank- p Burer–Monteiro factorizations for $O(r)$ optimization can approximate the full SDP relaxation in terms of *objective function value*. Their results bound the approximation error by a term proportional to r/p . Our results show that, in some cases, we already obtain perfect approximation with p only slightly larger than r .

An interesting parallel work on low-rank Burer–Monteiro factorization landscapes is [34]. However, their setting is quite different from ours (requiring a strongly convex objective and no constraints), so their results are not directly comparable.

2.2 The spectral approach and previous error bounds

Our work follows a large body of prior results that use spectral properties of the measurement graph. In particular, these results use the eigenvalues and eigenvectors of the graph Laplacian matrix L (or, in some cases, the adjacency matrix A) of the graph G . A particularly important quantity is the *graph connection Laplacian* matrix (defined in [35] for different purposes) which can be formed directly from our observations R_{ij} (this is precisely the matrix \widehat{L} in our notation—see Section 3 for the definition).

The *eigenvector method* was introduced in [36] for the purpose of rotation synchronization; this method directly uses the eigenvectors of the graph connection Laplacian (or, in the original paper, the adjacency matrix equivalent). Closely related to this, the paper [37] studies the relationship between the eigenvalues/vectors of the graph connection Laplacian and the optimal objective function value of (2).

The paper [38], by analyzing eigenvalues of \widehat{L} , provides conditions under which the SDP relaxation gives exact recovery for \mathbf{Z}_2 (i.e., $O(1)$) synchronization on an Erdős–Rényi graph. The paper [39] considers a robust version of the SDP relaxation that uses the sum of absolute errors rather than least-squares. They provide conditions for exact recovery for an Erdős–Rényi random graph and sparse errors.

The papers [4, 40, 26] and [41, Chapter 6] contain a variety of error bounds for the eigenvector method in terms of the graph Fiedler value $\lambda_2(L)$ and various norms of the measurement error matrix Δ . This is extended to $SE(r)$ synchronization (special Euclidean group) in [26]. These results are the most comparable to our error bounds, because they apply to general graphs and measurement errors. The bound in [26] is, within constants, identical to our bounds in Theorem 5 and Corollary 3.

The papers [42, 43, 27] show that the SDP relaxation, the (rounded) eigenvector method, and generalized power method (eigenvector method followed by iterative refinement) all achieve asymptotically minimax-optimal error with Gaussian noise on Erdős–Rényi random graphs (interestingly, [27], like the older paper [35], analyzes the adjacency matrix leading eigenvector). These results agree with our error bounds within constants (see Section 1.5.1), though our results apply to much more general situations.

2.3 Oscillator synchronization literature

Oscillator synchronization is a large field of research. See [44, 45] for surveys. Our work touches the small subset corresponding to simplified Kuramoto oscillators.

As discussed in Section 1.2, the classical and most well-studied Kuramoto oscillator is that of angular synchronization (i.e., on the unit circle S^1). One line of research studies *which connected graphs* synchronize on S^1 . This includes deterministic guarantees based on the density of a graph [46, 47, 17, 48, 49, 50] and high-probability properties of random graphs [47, 51, 13, 52]. For example, [50] shows that every graph synchronizes in which every vertex is connected to at least 3/4 of the other vertices. The paper [13] gives more general deterministic conditions based on spectral expander properties and shows that, asymptotically, Erdős–Rényi graphs that are connected also synchronize.

A complementary line of research studies *for which manifolds* do *all* connected oscillator networks synchronize. It was shown in [18, 19] that Kuramoto networks on the d -sphere S^d synchronize for any $d \geq 2$. This corresponds to the Stiefel manifold $\text{St}(r, p)$ for $r = 1$ and $p \geq 3$. More generally, the papers [15, 5] show that networks on $\text{St}(r, p)$ synchronize if $2p \geq 3(r + 1)$. Our Corollary 1 improves this condition to $p \geq r + 2$, which is optimal according to [53, 21] and confirms a conjecture in [5, 19]. See the discussion around Corollary 1 for further details. See also Section 1.3 for similar discussion in the complex case.

Oscillators on complex Stiefel manifolds can be seen as a generalization of the “quantum” Kuramoto oscillators introduced in [25]. See [44, 54] for more references.

3 Key mathematical tools

In this section, we make precise and fill out the mathematical framework for our analysis and results. We only consider the real case in this section and the next. We make the necessary adjustments for the complex case in Section 5.

3.1 Graph Laplacian formulation

In each optimization problem we consider, the orthogonality/block diagonal constraint ensures that the $r \times r$ diagonal blocks of the cost matrix C have no effect. We therefore replace C by another matrix that will be more convenient for analysis.

Let $A \in \mathbf{R}^{n \times n}$ be the adjacency matrix of G (i.e., the symmetric matrix with $A_{ij} = \mathbf{1}_{\{(i,j) \in E\}}$). Let L be the graph Laplacian matrix defined by

$$L_{ij} = \begin{cases} \sum_{k \neq i} A_{ik} & \text{if } i = j, \\ -A_{ij} & \text{if } i \neq j. \end{cases}$$

It is well known that L is a positive semidefinite (PSD) matrix whose smallest eigenvalue is $\lambda_1(L) = 0$ with corresponding eigenvector $v_1 = \mathbf{1}_n$. The measurement graph is connected if and only if the second-smallest eigenvalue $\lambda_2 = \lambda_2(L) > 0$.

Recall that $Z_1, \dots, Z_n \in \text{O}(r)$ are the ground-truth matrices that we want to estimate. Let

$$D = D(Z) := \begin{bmatrix} Z_1 & & & \\ & Z_2 & & \\ & & \ddots & \\ & & & Z_n \end{bmatrix}.$$

With \otimes denoting Kronecker product, let

$$L_Z := D(L \otimes I_r)D^\top \quad \text{and} \quad \widehat{L} := L_Z - \Delta,$$

where Δ is the symmetric matrix containing the measurement noise blocks Δ_{ij} (with $\Delta_{ij} = 0$ if $(i, j) \notin E$). Note that the eigenvalues of L_Z are identical to those of L (with multiplicities multiplied by r), and, if G is connected, the r -dimensional subspace corresponding to $\lambda_1(L) = 0$ is precisely the span of the columns of Z . The matrix \widehat{L} was introduced in [35] under the name *graph connection Laplacian*.

Note that $C_{ij} = -\widehat{L}_{ij}$ for $i \neq j$, and the diagonal blocks of the cost matrix have no effect on the optimization landscape of problems (3) and (4) due to the block diagonal constraint. Therefore, the SDP (3) has the exact same landscape in the variable X as

$$\min_{X \succeq 0} \langle \widehat{L}, X \rangle \text{ s.t. } X_{ii} = I_r, i = 1, \dots, n. \quad (13)$$

Likewise, the (relaxed) nonconvex problem (4) has the same landscape as

$$\min_{Y \in \mathbf{R}^{rn \times p}} \langle \widehat{L}, YY^\top \rangle \text{ s.t. } Y_i Y_i^\top = I_r, i = 1, \dots, n. \quad (14)$$

From now on, we use those formulations.

3.2 Manifold of feasible points and necessary optimality conditions

Optimization problems of the form (14) have been well studied. See, for example, [32, 7] for an overview. We summarize the relevant facts in this section.

First, note that the constraints in (13) and (14) apply to the $r \times r$ diagonal blocks of a matrix. To simplify notation, we denote the symmetric block-diagonal projection SBD: $\mathbf{R}^{rn \times rn} \rightarrow \mathbf{R}^{rn \times rn}$ by

$$\text{SBD}(X)_{ij} = \begin{cases} \frac{X_{ii} + X_{ii}^\top}{2} & \text{if } i = j, \\ 0 & \text{if } i \neq j. \end{cases}$$

We can then write the semidefinite problem (13) more compactly as

$$\min_{X \succeq 0} \langle \widehat{L}, X \rangle \text{ s.t. } \text{SBD}(X) = I_{rn}. \quad (15)$$

Similarly, we can write (14) as

$$\min_{Y \in \mathbf{R}^{rn \times p}} \langle \widehat{L}, YY^\top \rangle \text{ s.t. } \text{SBD}(YY^\top) = I_{rn}. \quad (16)$$

The *symmetrizing* aspect of the projection operator SBD is, for now, completely redundant but will become useful as we continue.

The feasible points of (16) form a smooth submanifold \mathcal{M} of $\mathbf{R}^{rn \times p}$:

$$\mathcal{M} := \text{St}(r, p)^n = \{Y \in \mathbf{R}^{rn \times p} : Y_i Y_i^\top = I_r \text{ for } i = 1, \dots, n\}.$$

The most important object for us to understand is the *tangent space* T_Y at a point $Y \in \mathcal{M}$. An $rn \times p$ matrix \dot{Y} is in T_Y if and only if its $r \times p$ blocks satisfy $\dot{Y}_i Y_i^\top + Y_i \dot{Y}_i^\top = 0 \in \mathbf{R}^{r \times r}$ for all $i = 1, \dots, n$. The orthogonal projection of an arbitrary $W \in \mathbf{R}^{rn \times p}$ onto T_Y is given by

$$\mathcal{P}_{T_Y}(W) = W - \text{SBD}(WY^\top)Y.$$

Local minima of (16) are also first- and second-order critical [7, Def. 2.3]: these conditions encode the fact that the Riemannian gradient is zero and the Riemannian Hessian is positive semidefinite (on the tangent space). To be specific, let

$$S(Y) := \widehat{L} - \text{SBD}(\widehat{L}YY^\top). \quad (17)$$

Then, one can show (see [7]) that any local minimum Y satisfies both of the following:

- First order condition: $S(Y)Y = 0$. This is proportional to the T_Y -projected gradient of the objective function.
- Second order condition: for all $\dot{Y} \in T_Y$, $\langle S(Y)\dot{Y}, \dot{Y} \rangle \geq 0$. This says that the Riemannian Hessian of the objective function is positive semidefinite.

A point Y that satisfies the first condition is a *first-order critical point*. A point Y that satisfies both conditions is a *second-order critical point*. Note that second-order criticality is independent of whether we write the problem as (4) or (16) (in fact, $S(Y)$ is unchanged if we replace \widehat{L} by $-C$).

3.3 Dual certificates and global optimality

A natural question that remains is the following: how do we know if a candidate solution Y to (16) is, in fact, globally optimal? This is a well-studied problem (again, see [7] for further discussion and references), and here we list some facts that will be useful throughout our analysis.

To study optimality conditions for (16), it is useful to consider the full SDP relaxation (15). To show that a feasible point X of (15) is optimal, it suffices to provide a *dual certificate*. For (15), a dual certificate is a matrix S of the form

$$S = \widehat{L} - \text{SBD}(\Lambda)$$

for some $rn \times rn$ matrix Λ with the conditions that (a) $S \succeq 0$ and (b) $\langle S, X \rangle = 0$ (or $SX = 0$, which is equivalent because $S, X \succeq 0$). If such a matrix S exists, we have, for any feasible point $X' \succeq 0$,

$$\begin{aligned} \langle \widehat{L}, X' \rangle - \langle \widehat{L}, X \rangle &= \langle \widehat{L}, X' - X \rangle \\ &= \langle S, X' - X \rangle + \langle \text{SBD}(\Lambda), X' - X \rangle \\ &= \langle S, X' \rangle - \underbrace{\langle S, X \rangle}_{=0} + \underbrace{\langle \Lambda, \text{SBD}(X' - X) \rangle}_{=0} = \langle S, X' \rangle \geq 0. \end{aligned}$$

Thus X is optimal. Furthermore, if X' is also optimal (i.e., equality holds above), we must have $SX' = 0$; we use this fact later.

To show that Y is a globally optimal solution to (16), it clearly suffices to show that YY^\top is an optimal solution to (15). Thus we want to find a dual certificate proving optimality of YY^\top . A natural candidate is the matrix $S(Y) = \widehat{L} - \text{SBD}(\widehat{L}YY^\top)$ from (17). First-order criticality implies that $S(Y)YY^\top = 0$. Thus it remains to show that $S(Y) \succeq 0$. We do this by leveraging the following fact (see, e.g., [7, Prop. 3.1]):

Lemma 1. *If Y is a second-order critical point of (16) that is rank deficient (i.e., $\text{rank}(Y) < p$), then $S(Y) \succeq 0$, and consequently YY^\top is an optimal solution to the SDP (15), and Y is a globally optimal solution to (16).*

This can be proved with an argument from [55]: if u is any unit-norm vector in the null space of Y , then, for any $z \in \mathbf{R}^{rn}$, $\dot{Y}(z) := zu^\top$ is in T_Y ; hence, second-order criticality implies

$$\langle S(Y)z, z \rangle = \langle S(Y)\dot{Y}(z), \dot{Y}(z) \rangle \geq 0.$$

Thus the key step in showing that Y is globally optimal is to show that it is *rank deficient*.

4 Proofs (real case)

We (still) denote by $\|A\|_{\ell_2}$, $\|A\|_{\text{F}}$, and $\|A\|_*$ the operator, Frobenius, and nuclear norms of a matrix A . Our proof strategy is as follows.

First, we show that each second-order critical point Y of (4) satisfies certain error bounds (Theorems 1 and 5). To do this, we can use inequalities of the form $\langle S(Y)\dot{Y}, \dot{Y} \rangle \geq 0$ for all $\dot{Y} \in T_Y$ —these

express the fact that the Riemannian Hessian at Y is positive semidefinite, with $S(Y)$ as in (17). We did not find a way to select a single \dot{Y} to prove our claims. Instead, the key enabling proof idea is this: we design a suitable probability distribution over the tangent space T_Y , and we exploit the fact that $\langle S(Y)\dot{Y}, \dot{Y} \rangle$ is still nonnegative *in expectation* over the random choice of \dot{Y} . This yields a valid inequality which may not be expressible using a single \dot{Y} .

Second, to prove our landscape results (Theorems 2 and 3), the critical step is to show that second-order critical points have low rank (after which we apply Lemma 1). To do this, we show (using the error bounds previously derived) that the matrix $S(Y)$ has *high* rank and then apply the first-order criticality condition $S(Y)Y = 0$.

To simplify notation in our proofs, we assume that $Z_i = I_r$ for all $i = 1, \dots, n$. This is without loss of generality because it can be arranged with a smooth and smoothly invertible change of variable. More explicitly, if Z is arbitrary (with $Z_i \in O(r)$), consider the change of variable $\pi: \mathcal{M} \rightarrow \mathcal{M}$ defined by $\pi(Y)_i = Z_i Y_i$. Since π is a Riemannian isometry, the landscapes of $F(Y) = \langle \hat{L}, YY^\top \rangle$ (16) and of $\bar{F} = F \circ \pi$ are the same [16, Prop. 9.6], in the sense that Y is first-order critical / second-order critical / locally optimal / globally optimal for \bar{F} if and only if $\pi(Y)$ is so for F . Using the definition of \hat{L} , the expression for \bar{F} simplifies to $\bar{F}(Y) = \langle L \otimes I_r - \bar{\Delta}, YY^\top \rangle$, where $\bar{\Delta}_{ij} = Z_i^\top \Delta_{ij} Z_j$. This is exactly F in the event that $Z_1 = \dots = Z_n = I_r$, including a change of variable on the noise matrix $\Delta \mapsto \bar{\Delta}$ which has no effect on its eigenvalues (hence on any of the claims we make about noise later on).

Accordingly, we proceed with the following simplified notation:

$$Z_i = I_r \quad \forall i, \quad D = I_{rn}, \quad L_Z = L \otimes I_r, \quad \hat{L} = L_Z - \Delta.$$

The next step is to design a distribution of random tangent vectors.

4.1 A distribution of random tangent vectors

We analyze critical points of (16). Recall from Section 3 that, setting $S(Y) = \hat{L} - \text{SBD}(\hat{L}YY^\top)$, a feasible point Y is first- and second-order critical if $S(Y)Y = 0$ and, for every $\dot{Y} \in T_Y$, $\langle S(Y), \dot{Y}\dot{Y}^\top \rangle \geq 0$. From here on, assume Y is such a point.

Recall that \dot{Y} is in T_Y if and only if $\dot{Y}_i Y_i^\top + Y_i \dot{Y}_i^\top = 0$ for $i = 1, \dots, n$. In other words, each $Y_i \dot{Y}_i^\top$ must be skew-symmetric. This is true if and only we can write

$$\dot{Y}_i = \Gamma_i (I - Y_i^\top Y_i) + S_i Y_i$$

for some $r \times p$ matrix Γ_i and some *skew-symmetric* $r \times r$ matrix S_i . The first term is the row-wise orthogonal projection of Γ_i onto $\text{null}(Y_i)$. If we choose $S_i = \Gamma_i Y_i^\top - Y_i \Gamma_i^\top$, we obtain

$$\dot{Y}_i = \Gamma_i - Y_i \Gamma_i^\top Y_i = Y_i (Y_i^\top \Gamma_i - \Gamma_i^\top Y_i).$$

In fact, this last formulation covers all possible \dot{Y}_i , because any $r \times r$ skew-symmetric matrix S_i can be written in the given form, and the components of Γ_i in $\text{range}(Y_i^\top)$ and $\text{null}(Y_i)$ can be chosen independently.

We choose a common $\Gamma_i = \Gamma$, where Γ is a random $r \times p$ matrix whose entries are i.i.d. standard normal random variables. This results in a random $\dot{Y} \in T_Y$ whose components $\dot{Y}_1, \dots, \dot{Y}_n$ are related. Because the second-order criticality inequality holds for *all* $\dot{Y} \in T_Y$, we can take an expectation to obtain

$$\langle S(Y), \mathbf{E} \dot{Y} \dot{Y}^\top \rangle = \mathbf{E} \langle S(Y), \dot{Y} \dot{Y}^\top \rangle \geq 0.$$

Simple calculations yield

$$\begin{aligned} \mathbf{E} \dot{Y}_i \dot{Y}_j^\top &= \mathbf{E} (\Gamma - Y_i \Gamma^\top Y_i) (\Gamma - Y_j \Gamma^\top Y_j)^\top \\ &= \mathbf{E} (\Gamma \Gamma^\top - Y_i \Gamma^\top Y_i \Gamma^\top - \Gamma Y_j^\top \Gamma Y_j^\top + Y_i \Gamma^\top Y_i Y_j^\top \Gamma Y_j^\top) \\ &= (p-2)I_r + \text{tr}(Y_i Y_j^\top) Y_i Y_j^\top. \end{aligned} \tag{18}$$

We have used the facts that (1) for any $r \times p$ matrix U , $\mathbf{E}\Gamma^\top U\Gamma^\top = U^\top$, and (2) for any $r \times r$ matrix B , $\mathbf{E}\Gamma^\top B\Gamma = \text{tr}(B)I_p$. When $i = j$, this simplifies to $\mathbf{E}\dot{Y}_i\dot{Y}_i^\top = (p+r-2)I_r$. This implies $\text{SBD}(\mathbf{E}\dot{Y}\dot{Y}^\top) = (p+r-2)I_{rn}$.

Using a random $\dot{Y} \in T_Y$ has appeared before in [33, 10]. Those papers chose (in our notation) $\dot{Y}_i = \Gamma(I - Y_i^\top Y_i)$, which is only the portion of Γ in $\text{null}(Y_i)$. Another similar approach to ours appears in [15, 5], where, rather than considering a random choice of \dot{Y} , the authors analyze the quadratic form $\Gamma \mapsto \langle S(Y), \dot{Y}(\Gamma)\dot{Y}(\Gamma)^\top \rangle$ with $\dot{Y}_i(\Gamma) = \mathcal{P}_{T_{Y_i}}(\Gamma)$. Their results do not use randomness and scale differently the portions of each \dot{Y}_i that are in $\text{null}(Y_i)$ and $\text{range}(Y_i^\top)$ (this is related to the choice of metric on the Stiefel manifold).

4.2 Noiseless case

For Theorem 1, we have $\Delta = 0$, so $\widehat{L} = L_Z = L \otimes I_r$, and $S(Y) = L_Z - \text{SBD}(L_Z Y Y^\top)$.

We first calculate

$$\begin{aligned} \langle \text{SBD}(\widehat{L} Y Y^\top), \mathbf{E}\dot{Y}\dot{Y}^\top \rangle &= \langle L_Z Y Y^\top, \text{SBD}(\mathbf{E}\dot{Y}\dot{Y}^\top) \rangle \\ &= (p+r-2) \text{tr}(L_Z Y Y^\top) \\ &= (p+r-2) \sum_{i,j=1}^n L_{ij} \text{tr}(Y_i Y_j^\top). \end{aligned}$$

Next, by (18), we derive

$$\begin{aligned} \langle L_Z, \mathbf{E}\dot{Y}\dot{Y}^\top \rangle &= \sum_{i,j=1}^n L_{ij} \langle I_r, \mathbf{E}\dot{Y}_i\dot{Y}_j^\top \rangle \\ &= \sum_{i,j=1}^n L_{ij} ((p-2)r + \text{tr}^2(Y_i Y_j^\top)) \\ &= \sum_{i,j=1}^n L_{ij} \text{tr}^2(Y_i Y_j^\top), \end{aligned}$$

where the last equality follows from the fact that $\sum_i L_{ij} = 0$ for all j .

To proceed, note that

$$Y_i Y_j^\top + Y_j Y_i^\top = 2I_r - (Y_i - Y_j)(Y_i - Y_j)^\top,$$

so that

$$\text{tr}(Y_i Y_j^\top) = \frac{1}{2} \text{tr}(Y_i Y_j^\top + Y_j Y_i^\top) = r - \frac{1}{2} \|Y_i - Y_j\|_{\mathbb{F}}^2. \quad (19)$$

We then find (again using the fact that all rows and columns of L sum to zero)

$$\begin{aligned} \langle L_Z, \mathbf{E}\dot{Y}\dot{Y}^\top \rangle &= \sum_{i,j=1}^n L_{ij} \left(r - \frac{1}{2} \|Y_i - Y_j\|_{\mathbb{F}}^2 \right)^2 \\ &= -r \sum_{i,j=1}^n L_{ij} \|Y_i - Y_j\|_{\mathbb{F}}^2 + \frac{1}{4} \sum_{i,j=1}^n L_{ij} \|Y_i - Y_j\|_{\mathbb{F}}^4 \\ &= 2r \sum_{i,j=1}^n L_{ij} \text{tr}(Y_i Y_j^\top) - \frac{1}{4} \sum_{i,j=1}^n A_{ij} \|Y_i - Y_j\|_{\mathbb{F}}^4. \end{aligned}$$

All combined, the condition $\langle S(Y), \mathbf{E} \dot{Y} \dot{Y}^\top \rangle \geq 0$ then implies

$$(p-r-2) \sum_{i,j=1}^n L_{ij} \operatorname{tr}(Y_i Y_j^\top) + \frac{1}{4} \sum_{i,j=1}^n A_{ij} \|Y_i - Y_j\|_{\mathbb{F}}^4 \leq 0. \quad (20)$$

The second term on the left-hand side is nonnegative. If $p \geq r+2$, the first term is also nonnegative (the sum equals $\langle L_Z, Y Y^\top \rangle$). Therefore, both terms on the left-hand side of (20) must be 0, so $Y_i = Y_j$ for all $(i, j) \in E$. If G is connected, this implies that the Y_i 's are identical, and therefore

$$\langle Z Z^\top, Y Y^\top \rangle = \|Z^\top Y\|_{\mathbb{F}}^2 = \|n Y_1\|_{\mathbb{F}}^2 = n^2 r.$$

This finishes the proof of Theorem 1.

When $p = r+2$, the robustness to (small) perturbations comes from the quartic terms in (20). This robustness is much weaker than what we prove in Section 4.3 for the noisy results (where we use the *quadratic* terms that arise when $p > r+2$).

4.3 Noisy case

We now consider the case where the noise matrix Δ is nonzero. We prove Theorem 5 first (high correlation) and then use it to prove Theorems 2 and 3 (global optimality).

To aid our analysis, we write $Y = ZR + W$, with $R = \frac{1}{n} Z^\top Y \in \mathbf{R}^{r \times p}$ and W orthogonal to Z (i.e., $Z^\top W = \sum_i W_i = 0$). This gives $Y_i = R + W_i$. Note that

$$\|Z^\top Y\|_{\mathbb{F}}^2 = \|nR\|_{\mathbb{F}}^2 = n \|ZR\|_{\mathbb{F}}^2 = n^2 r - n \|W\|_{\mathbb{F}}^2. \quad (21)$$

Thus, we set out to use second-order criticality of Y to infer that $\|W\|_{\mathbb{F}}$ is small.

4.3.1 Error bound for all second-order critical points

The second-order criticality condition is now, for all $\dot{Y} \in T_Y$,

$$\langle L_Z - \Delta, \dot{Y} \dot{Y}^\top \rangle - \langle \text{SBD}((L_Z - \Delta) Y Y^\top), \dot{Y} \dot{Y}^\top \rangle \geq 0. \quad (22)$$

We use the same random \dot{Y} as in the previous section. We have already analyzed the terms involving L_Z in Section 4.2, so it remains to analyze the terms involving Δ .

Note that because we have assumed that every $Z_i = I_r$, we have

$$\sum_{i,j=1}^n \langle \Delta_{ij}, I_r \rangle = \sum_{i,j=1}^n \langle \Delta_{ij}, Z_i Z_j^\top \rangle = \langle \Delta, Z Z^\top \rangle. \quad (23)$$

From (18), we calculate

$$\begin{aligned} \langle \Delta, \mathbf{E} \dot{Y} \dot{Y}^\top \rangle &= \sum_{i,j=1}^n \langle \Delta_{ij}, (p-2)I_r + \operatorname{tr}(Y_i Y_j^\top) Y_i Y_j^\top \rangle \\ &= (p-2) \langle \Delta, Z Z^\top \rangle + \sum_{i,j=1}^n \left(r - \frac{1}{2} \|Y_i - Y_j\|_{\mathbb{F}}^2 \right) \langle \Delta_{ij}, Y_i Y_j^\top \rangle \\ &= (p-2) \langle \Delta, Z Z^\top \rangle + r \langle \Delta, Y Y^\top \rangle - \frac{1}{2} \sum_{i,j=1}^n \|Y_i - Y_j\|_{\mathbb{F}}^2 \langle \Delta_{ij}, Y_i Y_j^\top \rangle. \end{aligned}$$

The second equality uses (19) and (23). Next, $\text{SBD}(\mathbf{E} \dot{Y} \dot{Y}^\top) = (p+r-2)I_{rn}$ implies

$$\langle \text{SBD}(\Delta Y Y^\top), \mathbf{E} \dot{Y} \dot{Y}^\top \rangle = (p+r-2) \langle \Delta, Y Y^\top \rangle.$$

The difference is

$$\begin{aligned}
& \langle \text{SBD}(\Delta YY^\top), \mathbf{E} \dot{Y} \dot{Y}^\top \rangle - \langle \Delta, \mathbf{E} \dot{Y} \dot{Y}^\top \rangle \\
&= (p-2) \langle \Delta, YY^\top - ZZ^\top \rangle + \sum_{i,j=1}^n \left\langle \Delta_{ij}, \frac{1}{2} \|Y_i - Y_j\|_{\mathbb{F}}^2 Y_i Y_j^\top \right\rangle \\
&= (p-2) \langle \Delta, YY^\top - ZZ^\top \rangle + \langle \Delta, (Q \otimes \mathbf{1}_r \mathbf{1}_r^\top) \circ (YY^\top) \rangle, \tag{24}
\end{aligned}$$

where \circ is entrywise product and $Q_{ij} = \frac{1}{2} \|Y_i - Y_j\|_{\mathbb{F}}^2$.

We aim to bound (in nuclear norm) the matrices that are in an inner product with Δ . Note that the $r \times r$ blocks of $YY^\top - ZZ^\top$ are

$$(YY^\top - ZZ^\top)_{ij} = Y_i Y_j^\top - I_r = Y_i (Y_j - Y_i)^\top = Y_i (W_j - W_i)^\top,$$

so we can write $YY^\top - ZZ^\top = YW^\top - H$, where $H_{ij} = Y_i W_i^\top$. By the matrix Hölder inequality for Schatten p -norms, $\|YW^\top\|_* \leq \|Y\|_{\mathbb{F}} \|W\|_{\mathbb{F}} = \sqrt{rn} \|W\|_{\mathbb{F}}$. Furthermore,

$$H = \begin{bmatrix} Y_1 W_1^\top \\ \vdots \\ Y_n W_n^\top \end{bmatrix} Z^\top.$$

Because each Y_i has operator norm 1, the left factor in the above expression has Frobenius norm at most $\|W\|_{\mathbb{F}}$. Also, $\|Z\|_{\mathbb{F}} = \sqrt{rn}$. Thus $\|H\|_* \leq \sqrt{rn} \|W\|_{\mathbb{F}}$. We conclude that $\|YY^\top - ZZ^\top\|_* \leq 2\sqrt{nr} \|W\|_{\mathbb{F}}$.

We also need a bound on

$$\|(Q \otimes \mathbf{1}_r \mathbf{1}_r^\top) \circ (YY^\top)\|_* \stackrel{(a)}{\leq} \|(Q \otimes \mathbf{1}_r \mathbf{1}_r^\top)\|_* \stackrel{(b)}{=} r \|Q\|_*.$$

Inequality (a) follows from a basic inequality on singular values of Hadamard products [56, Thm. 5.6.2], using the fact that each row of Y has norm 1. Equality (b) follows from the eigenvalue characterization of Kronecker products. To bound $\|Q\|_*$, note that Q_{ij} is simply the trace of the (i, j) th block of $ZZ^\top - YY^\top$. Thus Q is a partial trace of $ZZ^\top - YY^\top$, and therefore (see [57]) $\|Q\|_* \leq \|ZZ^\top - YY^\top\|_* \leq 2\sqrt{nr} \|W\|_{\mathbb{F}}$.

Putting all the nuclear norm bounds together, we obtain, by Hölder's inequality for matrix inner products applied on (24) (von Neumann's trace inequality),

$$\langle \text{SBD}(\Delta YY^\top), \mathbf{E} \dot{Y} \dot{Y}^\top \rangle - \langle \Delta, \mathbf{E} \dot{Y} \dot{Y}^\top \rangle \leq 2(p+r-2) \|\Delta\|_{\ell_2} \sqrt{rn} \|W\|_{\mathbb{F}}.$$

Combining this with (22) and the calculations of Section 4.2, we obtain

$$(p-r-2) \sum_{i,j} L_{ij} \langle Y_i, Y_j \rangle + \frac{1}{4} \sum_{i,j=1}^n A_{ij} \|W_i - W_j\|_{\mathbb{F}}^4 \leq 2(p+r-2) \|\Delta\|_{\ell_2} \sqrt{rn} \|W\|_{\mathbb{F}}. \tag{25}$$

Dropping the nonnegative quartic terms and using the fact that

$$\sum_{i,j} L_{ij} \langle Y_i, Y_j \rangle = \sum_{i,j} L_{ij} \langle W_i, W_j \rangle \geq \lambda_2 \|W\|_{\mathbb{F}}^2$$

(where $\lambda_2 = \lambda_2(L)$ is the Fiedler value of G), we get

$$(p-r-2) \lambda_2 \|W\|_{\mathbb{F}}^2 \leq 2(p+r-2) \|\Delta\|_{\ell_2} \sqrt{rn} \|W\|_{\mathbb{F}}.$$

Therefore,

$$\|W\|_{\mathbb{F}}^2 \leq \left(\frac{2(p+r-2) \|\Delta\|_{\ell_2}}{(p-r-2) \lambda_2} \right)^2 rn = C_p^2 rn \frac{\|\Delta\|_{\ell_2}^2}{\lambda_2^2}. \tag{26}$$

Combining this with the identities (21) finishes the proof of Theorem 5.

4.3.2 Bound on solution rank

We next prove Theorem 2. To show that a second-order critical point Y has low rank, recall that the first-order criticality condition states $S(Y)Y = 0$. Therefore, it suffices to show that $S(Y)$ has high rank. Recall

$$S(Y) = \widehat{L} - \text{SBD}(\widehat{L}YY^\top) = L_Z - \Delta - \text{SBD}(L_ZYY^\top) + \text{SBD}(\Delta YY^\top).$$

Because G is connected, λ_2 is positive. Thus L_Z has an r -dimensional null space, and its remaining $(n-1)r$ eigenvalues are at least λ_2 . Assume $\|\Delta\|_{\ell_2} < \lambda_2$ (as otherwise the theorem statement is true but vacuous). Given a matrix A , let $\sigma_k(A)$ denote its k th singular value, in decreasing order. To bound the rank of Y , we count how many singular values of $S(Y)$ can possibly be equal to zero. Explicitly, for any $c \in (0, 1)$, it holds (see the explanation below):

$$\begin{aligned} \text{rank}(Y) &\leq \dim \text{null}(S(Y)) \\ &\leq r + |\{\ell : \sigma_\ell(\text{SBD}(L_ZYY^\top) - \text{SBD}(\Delta YY^\top)) \geq \lambda_2 - \|\Delta\|_{\ell_2}\}| \\ &\leq r + |\{\ell : \sigma_\ell(\text{SBD}(L_ZYY^\top)) \geq c(\lambda_2 - \|\Delta\|_{\ell_2})\}| \\ &\quad + |\{\ell : \sigma_\ell(\text{SBD}(\Delta YY^\top)) \geq (1-c)(\lambda_2 - \|\Delta\|_{\ell_2})\}| \\ &\leq r + \frac{\|\text{SBD}(L_ZYY^\top)\|_*}{c(\lambda_2 - \|\Delta\|_{\ell_2})} + \frac{\|\text{SBD}(\Delta YY^\top)\|_{\text{F}}^2}{(1-c)^2(\lambda_2 - \|\Delta\|_{\ell_2})^2}. \end{aligned} \quad (27)$$

The third inequality is an application of the following fact: if matrices A and B (of the same size) have, respectively, at most k_A singular values larger than M_A and k_B singular values larger than M_B , then $A+B$ has at most k_A+k_B singular values larger than M_A+M_B . This follows from [56, Thm. 3.3.16], which implies $\sigma_{k_A+k_B+1}(A+B) \leq \sigma_{k_A+1}(A) + \sigma_{k_B+1}(B) < M_A + M_B$.

To bound this last quantity, first note that, because $\|Y_i\|_{\ell_2} = 1$ for each i ,

$$\|\text{SBD}(\Delta YY^\top)\|_{\text{F}}^2 \leq \sum_i \|(\Delta Y)_i Y_i^\top\|_{\text{F}}^2 \leq \|\Delta Y\|_{\text{F}}^2 \leq \|\Delta\|_{\ell_2}^2 \|Y\|_{\text{F}}^2 = rn \|\Delta\|_{\ell_2}^2. \quad (28)$$

Next, using $L_Z = L \otimes I_r$, note that

$$\begin{aligned} (\text{SBD}(L_ZYY^\top))_{ii} &= \frac{1}{2} \sum_{j=1}^n L_{ij} (Y_i Y_j^\top + Y_j Y_i^\top) \\ &= \sum_{j=1}^n L_{ij} \left(I_r - \frac{1}{2} (Y_i - Y_j)(Y_i - Y_j)^\top \right) \\ &= \frac{1}{2} \sum_{j=1}^n A_{ij} (Y_i - Y_j)(Y_i - Y_j)^\top \\ &\succeq 0. \end{aligned}$$

Therefore, $\text{SBD}(L_ZYY^\top)$ is positive semidefinite and it follows that its nuclear norm is bounded as:

$$\begin{aligned} \|\text{SBD}(L_ZYY^\top)\|_* &= \text{tr}(\text{SBD}(L_ZYY^\top)) \\ &= \sum_{i,j=1}^n L_{ij} \text{tr}(Y_i Y_j^\top) \\ &\stackrel{(i)}{\leq} C_p \|\Delta\|_{\ell_2} \sqrt{rn} \|W\|_{\text{F}} \\ &\stackrel{(ii)}{\leq} C_p^2 rn \frac{\|\Delta\|_{\ell_2}^2}{\lambda_2}. \end{aligned} \quad (29)$$

Inequality (i) comes from (25) in the proof of Theorem 5. Inequality (ii) follows from the bound on $\|W\|_F$ provided by (26) in that same proof.

Plugging (28) and (29) into (27), we obtain

$$\text{rank}(Y) \leq r + \left(\frac{C_p^2}{c\lambda_2(\lambda_2 - \|\Delta\|_{\ell_2})} + \frac{1}{(1-c)^2(\lambda_2 - \|\Delta\|_{\ell_2})^2} \right) \|\Delta\|_{\ell_2}^2 rn.$$

Assume $\|\Delta\|_{\ell_2} \leq \lambda_2/4$. Choosing $c = 1/2$ and using the fact that $C_p \geq 2$, we see that

$$\text{rank}(Y) \leq r + \left(\frac{8}{3} \frac{C_p^2}{\lambda_2^2} + \frac{64}{9} \frac{1}{\lambda_2^2} \right) \|\Delta\|_{\ell_2}^2 rn \leq r + 5 \left(\frac{C_p \|\Delta\|_{\ell_2}}{\lambda_2} \right)^2 rn.$$

That last bound still holds if $\|\Delta\|_{\ell_2} > \lambda_2/4$ since $\text{rank}(Y) \leq rn$. This completes the rank-bound portion of Theorem 2. If p is larger than this rank bound, then Y is rank-deficient, and we apply Lemma 1 to obtain the rest of the result.

A limiting factor in how small we must make $\|\Delta\|_{\ell_2}$ in the above proof is the need to bound the singular values of $\text{SBD}(L_Z Y Y^\top)$. If G is the complete graph, $L_Z = I_{rn} - Z Z^\top$, so

$$S(Y) = \text{SBD}((Z Z^\top + \Delta) Y Y^\top) - Z Z^\top - \Delta.$$

Here it suffices to *lower bound* the singular values of the first term, and there is no need to bound $\text{SBD}(L_Z Y Y^\top)$. This simplification allows existing work (e.g., [10]) to obtain better results in the complete-graph case (with additional assumptions on Δ). It is not clear how to analyze a general graph G in such a way that we recover existing results when G is complete.

4.3.3 Solution uniqueness

To prove Theorem 3, note that, under the assumptions of Theorem 3, Theorem 2 and its proof imply that $\text{rank}(S(Y)) \geq rn - r$ and, by first-order criticality, $\text{rank}(Y) \leq r$. These rank inequalities are, in fact, equalities, because the constraint $Y_1 Y_1^\top = I_r$ implies $\text{rank}(Y) \geq r$. Thus $\text{rank}(S(Y)) = rn - r$, and $\text{rank}(Y) = r$.

Since $p > r$, Lemma 1 again implies that $Y Y^\top$ solves the SDP (15), and $S(Y) \succeq 0$ is its dual certificate. We set out to prove that $Y Y^\top$ is the *unique* solution. First, note that because Y has rank r we can write $Y = \widehat{Z} U$, with $\widehat{Z} \in \mathbf{O}(r)^n$ and $U \in \mathbf{R}^{r \times p}$ such that $U U^\top = I_r$. Then $Y Y^\top = \widehat{Z} \widehat{Z}^\top$. Furthermore, as discussed in Section 3.3, *any* optimal solution X of the SDP must satisfy $S(Y) X = 0$. Because the columns of \widehat{Z} span the kernel of $S(Y)$, we can write $X = (\widehat{Z} B)(\widehat{Z} B)^\top = \widehat{Z} (B B^\top) \widehat{Z}^\top$ for some $r \times r$ matrix B . The block-diagonal constraint implies that

$$0 = (Y Y^\top - X)_{11} = (\widehat{Z} \widehat{Z}^\top - \widehat{Z} (B B^\top) \widehat{Z}^\top)_{11} = Z_1 (I_r - B B^\top) Z_1^\top.$$

Because $Z_1 \in \mathbf{O}(r)$, we must have $B B^\top = I_r$, and therefore $X = Y Y^\top$. Thus $Y Y^\top = \widehat{Z} \widehat{Z}^\top$ is the *unique* SDP solution.

The fact that $Y Y^\top = \widehat{Z} \widehat{Z}^\top$ is the optimal solution to (15) (and therefore of (3)) implies that \widehat{Z} and Y are, respectively, global optima of (2) and (4). For uniqueness, note that for any other global optima Z' of (2) and Y' of (4), $Z' Z'^\top$ and $Y' Y'^\top$ are feasible points of (3) with the same objective function value as $\widehat{Z} \widehat{Z}^\top = Y Y^\top$. Therefore, by the uniqueness of the SDP solution, we have $Z' Z'^\top = Y' Y'^\top = Y Y^\top = \widehat{Z} \widehat{Z}^\top$, implying that $Z' = \widehat{Z}$ and $Y' = Y$ up to global orthogonal transformations. This completes the proof of Theorem 3.

5 Extension of proofs to the complex case

We extend the previous section's argument to the complex case in a direct way, only considering noiseless measurements. This yields the apparently new yet possibly suboptimal result stated in

Theorem 4. We simply substitute complex quantities for real ones in the previous arguments, replacing transposes (A^\top) by their Hermitian counterparts (A^*). To avoid ambiguity, we will define the matrix inner product as $\langle A, B \rangle = \text{real}(\text{tr}(AB^*))$, writing out the trace explicitly when we need to consider its imaginary part.

We still assume, without loss of generality, that $Z_1 = \dots = Z_n = I_r$, so that $\widehat{L} = L_Z = L \otimes I_r$ in the noiseless case. Once again, we use the fact that the Riemannian Hessian is PSD at a second-order critical point. Similarly to (17), we now take $S(Y) = \widehat{L} - \text{SBD}(\widehat{L}YY^*)$, where SBD now keeps the *Hermitian* part of the $r \times r$ diagonal blocks (again making the off-diagonal blocks zero). Second-order criticality means that $S(Y)Y = 0$ and $\langle S(Y), \dot{Y}\dot{Y}^* \rangle \geq 0$ for all \dot{Y} in the tangent space at $Y \in \text{St}(r, p, \mathbf{C})^n$. Details appear in [58].

For the time being (we shall modify this later in this section), we directly translate the construction in Section 4.1 and choose tangent vectors $\dot{Y}_i = \Gamma - Y_i\Gamma^*Y_i$ to the points $Y_i \in \text{St}(p, r, \mathbf{C})$, where now Γ is an $r \times p$ matrix of i.i.d. *complex* standard normal random variables. This is indeed tangent as $\dot{Y}_iY_i^* + Y_i\dot{Y}_i^* = 0$. By a similar calculation to before,

$$\begin{aligned} \mathbf{E} \dot{Y}_i \dot{Y}_j^* &= \mathbf{E}(\Gamma\Gamma^* - Y_i\Gamma^*Y_i\Gamma^* - \Gamma Y_j^*\Gamma Y_j^* + Y_i\Gamma^*Y_iY_j^*\Gamma Y_j^*) \\ &= pI_r + \text{tr}(Y_iY_j^*)Y_iY_j^*. \end{aligned}$$

The first difference from the real case is that the terms with two factors of Γ or Γ^* have zero expectation, because each entry in these terms is a polynomial in standard complex normal random variables and thus is radially symmetric.¹³ Note that $\mathbf{E} \dot{Y}_i \dot{Y}_i^* = (p+r)I_r$. First, we can compute, similarly to before,

$$\langle \text{SBD}(L_Z YY^*), \mathbf{E} \dot{Y}\dot{Y}^* \rangle = (p+r) \sum_{i,j=1}^n L_{ij} \langle Y_i, Y_j \rangle. \quad (30)$$

Next, we have (see Section 4.2)

$$\langle L_Z, \mathbf{E} \dot{Y}\dot{Y}^* \rangle = \sum_{i,j=1}^n \text{real}(\text{tr}^2(Y_iY_j^*)). \quad (31)$$

We now come to the second significant difference from the real case: the calculation (19) fails here, because $\text{tr}(Y_iY_j^*)$ is not necessarily real.¹⁴ By considering the real and imaginary parts of $\text{tr}(Y_iY_j^*)$, we obtain

$$\langle L_Z, \mathbf{E} \dot{Y}\dot{Y}^* \rangle = \frac{1}{4} \sum_{i,j=1}^n L_{ij} [\text{tr}^2(Y_iY_j^* + Y_jY_i^*) - |\text{tr}(Y_iY_j^* - Y_jY_i^*)|^2]. \quad (32)$$

The first term can be handled akin to (19) in the real case. The optimal way to handle the second term is unclear. One way is to use $|\text{tr}(A)|^2 \leq \|A\|_*^2 \leq r\|A\|_{\mathbb{F}}^2$ (twice) and $\|A + A^*\|_{\mathbb{F}}^2 + \|A - A^*\|_{\mathbb{F}}^2 = 4\|A\|_{\mathbb{F}}^2$ to show that

$$\begin{aligned} |\text{tr}(Y_iY_j^* - Y_jY_i^*)|^2 &\leq r\|Y_iY_j^* - Y_jY_i^*\|_{\mathbb{F}}^2 \\ &= 4r\|Y_iY_j^*\|_{\mathbb{F}}^2 - r\|Y_iY_j^* + Y_jY_i^*\|_{\mathbb{F}}^2 \\ &\leq 4r\|Y_iY_j^*\|_{\mathbb{F}}^2 - \text{tr}^2(Y_iY_j^* + Y_jY_i^*). \end{aligned} \quad (33)$$

Both sides of the above inequality are zero when $i = j$. For $i \neq j$, recall that $L_{ij} \leq 0$. Therefore,

$$\langle L_Z, \mathbf{E} \dot{Y}\dot{Y}^* \rangle \leq \frac{1}{4} \sum_{i,j=1}^n L_{ij} [2\text{tr}^2(Y_iY_j^* + Y_jY_i^*) - 4r\|Y_iY_j^*\|_{\mathbb{F}}^2]. \quad (34)$$

¹³If z is a standard normal random variable (scalar), then in the real case $\mathbf{E} z^2 = 1$ but in the complex case $\mathbf{E} z^2 = 0$.

¹⁴If we ignored this issue, we could immediately “prove” that $p = r$ suffices to obtain a benign landscape. This is clearly false, as the case $r = 1$ (angular synchronization) demonstrates.

Additionally, $\sum_{i,j} L_{ij} \|Y_i Y_j^*\|_{\mathbb{F}}^2 = \sum_{i,j} L_{ij} \langle Y_i^* Y_i, Y_j^* Y_j \rangle \geq 0$, hence we can remove the last term while preserving the inequality. We now combine this and (30) into the inequality $\langle S(Y), \mathbf{E} \dot{Y} \dot{Y}^* \rangle \geq 0$ to obtain

$$\begin{aligned} (p+r) \sum_{i,j=1}^n L_{ij} \langle Y_i, Y_j \rangle &\leq \frac{1}{2} \sum_{i,j=1}^n L_{ij} \operatorname{tr}^2(Y_i Y_j^* + Y_j Y_i^*) \\ &= 4r \sum_{i,j=1}^n L_{ij} \langle Y_i, Y_j \rangle - \frac{1}{2} \sum_{i,j=1}^n A_{ij} \|Y_i - Y_j\|_{\mathbb{F}}^4. \end{aligned}$$

(The equality follows just as in the real case, e.g., by (19).)

This latter inequality yields perfect recovery provided $p \geq 3r$. This condition seems much worse than what we obtained in the real case.

We can improve the result by making a slightly different choice of the \dot{Y}_i 's. Note that we can write our choice as

$$\dot{Y}_i = \Gamma - Y_i \Gamma^* Y_i = \Gamma(I_p - Y_i^* Y_i) + (\Gamma Y_i^* - Y_i \Gamma^*) Y_i.$$

The first term has rows orthogonal to Y_i , while the second has a skew-symmetric matrix left-multiplying Y_i (rather than right-multiplying as before): both terms are therefore tangent vectors. We can rescale them arbitrarily, as

$$\dot{Y}_i = a\Gamma(I_p - Y_i^* Y_i) + b(\Gamma Y_i^* - Y_i \Gamma^*) Y_i$$

for any numbers $a \in \mathbf{C}$ and $b \in \mathbf{R}$. For $a, b > 0$ (which turns out to be the only sensible choice), this is related to the choice of metric on the Stiefel manifold. We choose $a = 2$ and $b = 1$, which makes \dot{Y} the (Euclidean) orthogonal projection of $2Z\Gamma$ onto T_Y . Intrinsically, this is quite similar to a complex adaptation of the proof in [5], though that argument is not phrased in terms of randomness. Now, for Γ chosen randomly as before,

$$\begin{aligned} \mathbf{E} \dot{Y}_i \dot{Y}_j^* &= 4\mathbf{E} \Gamma(I_p - Y_i^* Y_i)(I_p - Y_j^* Y_j) \Gamma^* + \mathbf{E}(\Gamma Y_i^* - Y_i \Gamma^*) Y_i Y_j^* (Y_j \Gamma^* - \Gamma Y_j^*) \\ &\quad + 2\mathbf{E} \Gamma(I_p - Y_i^* Y_i) Y_j^* (Y_j \Gamma^* - \Gamma Y_j^*) + 2\mathbf{E}(\Gamma Y_i^* - Y_i \Gamma^*) Y_i (I_p - Y_j^* Y_j) \Gamma^* \\ &= 4\langle I_p - Y_i^* Y_i, I_p - Y_j^* Y_j \rangle I_r + \langle Y_i^* Y_i, Y_j^* Y_j \rangle I_r + \operatorname{tr}(Y_i Y_j^*) Y_i Y_j^* \\ &\quad + 2\langle I_p - Y_i^* Y_i, Y_j^* Y_j \rangle I_r + 2\langle Y_i^* Y_i, I_p - Y_j^* Y_j \rangle I_r \\ &= (4(p-r) + \|Y_i Y_j^*\|_{\mathbb{F}}^2) I_r + \operatorname{tr}(Y_i Y_j^*) Y_i Y_j^*. \end{aligned}$$

We have used the fact that $\operatorname{tr}(AB^*)$ is always real when A and B are Hermitian. Similar calculations as before, combined with (33), yield

$$\begin{aligned} (4p-2r) \sum L_{ij} \langle Y_i, Y_j \rangle &\leq \sum L_{ij} (r \|Y_i Y_j^*\|_{\mathbb{F}}^2 + \operatorname{tr}^2(Y_i Y_j^*)) \\ &\leq \sum L_{ij} \left(r \|Y_i Y_j^*\|_{\mathbb{F}}^2 + \frac{1}{2} \operatorname{tr}^2(Y_i Y_j^* + Y_j Y_i^*) - r \|Y_i Y_j^*\|_{\mathbb{F}}^2 \right) \\ &= 4r \sum L_{ij} \langle Y_i, Y_j \rangle - \frac{1}{2} \sum A_{ij} \|Y_i - Y_j\|_{\mathbb{F}}^4. \end{aligned}$$

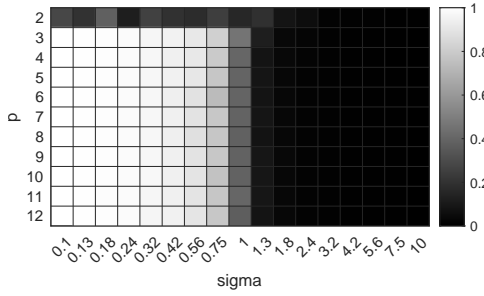
Thus, if G is connected, $2p \geq 3r$ implies $Y_1 = \dots = Y_n$, or, equivalently, $YY^* = ZZ^*$. The key benefit to this choice of \dot{Y} is that we exactly cancel (rather than drop) the $\|Y_i Y_j^*\|_{\mathbb{F}}^2$ terms that arise in (33).

6 Simulations

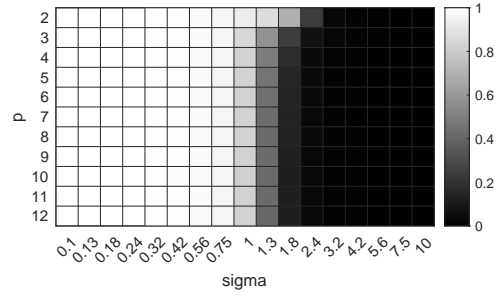
We implemented¹⁵ an algorithm for solving (4) and ran experiments on several graphs. We used Matlab with the Manopt toolbox [59] to optimize over a product of Stiefel manifolds with the default second-order trust-region algorithm.

We ran experiments on three graphs:

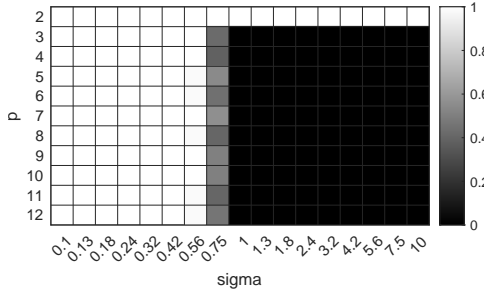
¹⁵Our code is available online at https://github.com/admcrae/sync_relaxed.



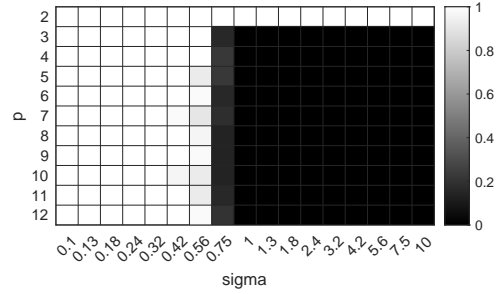
(a) Normalized correlation $\|Z^\top Y\|_F^2/n^2r$



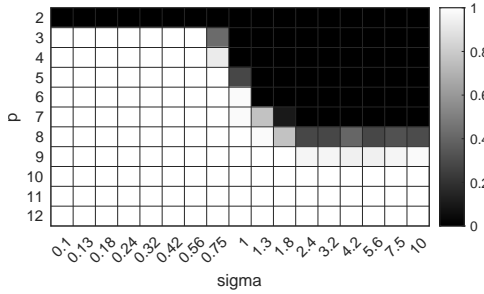
(a) Normalized correlation $\|Z^\top Y\|_F^2/n^2r$



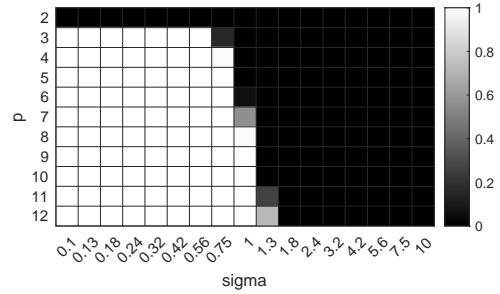
(b) Solution is rank- r



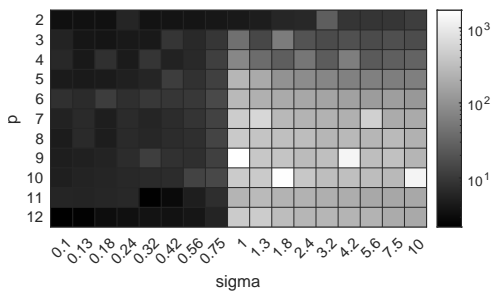
(b) Solution is rank- r



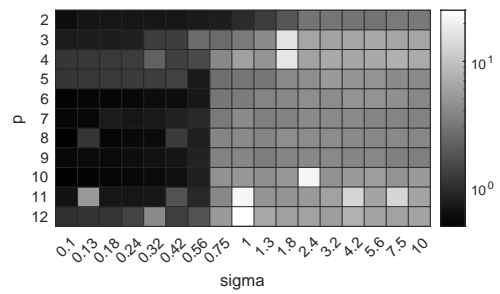
(c) Solution is rank-deficient



(c) Solution is rank-deficient



(d) Solve time (s)



(d) Solve time (s)

Figure 2: Experiments ($r = 2$) with a circulant graph on $n = 400$ vertices, each vertex having degree 10. All values are the average of 50 experiments.

Figure 3: Experiments ($r = 2$) on a graph on $n = 400$ vertices chosen from an ER model with average degree 10. All values are the average of 50 experiments.

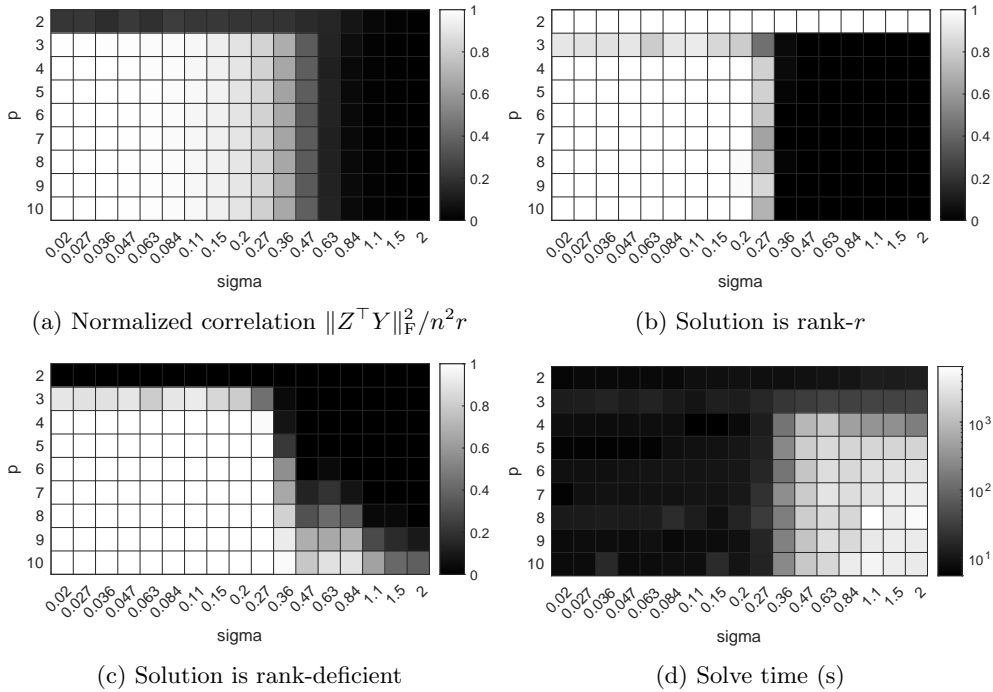


Figure 4: Experiments ($r = 2$) on the `fr079` SLAM dataset pose graph with $n = 989$ vertices of average degree 3.4. All values are the average of 50 experiments.

1. A circulant graph on 400 vertices, each having degree 10 (results in Figure 2). This graph topology is known to have spurious local minima (see, e.g., [17]).
2. A single realization of the Erdős–Rényi random graph on 400 vertices, each vertex having expected degree 10 (Figure 3). Because Erdős–Rényi graphs behave spectrally much like complete graphs, we expect them to be less prone to spurious local minima than the circulant graph (see [13]).
3. The pose graph from the Freiburg Building 079 (`fr079`) SLAM dataset in robotics,¹⁶ which has 989 vertices with average degree 3.4 (Figure 4).

All experiments are in the real number case and use $r = 2$. Theorem 1 predicts that, in the noiseless case, we should see benign nonconvexity for $p \geq 4$. All experiments use random noise and initialization. In the case $p = r = 2$, the initial point is chosen to be in the same connected component as the ground truth. The noise matrix Δ is chosen with i.i.d. $\mathcal{N}(0, \sigma^2)$ entries in the nonzero blocks (with the constraint $\Delta = \Delta^\top$). The reported $\text{rank}(Y)$ is the number of singular values that are at least $10^{-3}\sqrt{n}$ (note that Z 's nonzero singular values are all \sqrt{n}). The singular value tolerance did not qualitatively change the results (there was only a very slight effect at the phase transition).

The results are summarized in Figures 2 to 4. A few features worth highlighting are the following:

- There is a clear phase transition as the noise standard deviation σ increases; for each graph, the correlation performance, solution rank, and algorithm runtime all change dramatically in approximately the same place.
- The estimates cease to be rank- r at only slightly lower noise levels than where the recovery performance noticeably begins to degrade. This suggests that, for these experiments, the prediction

¹⁶Recorded by Cyrill Stachniss and available at <https://www.ipb.uni-bonn.de/datasets/>.

of Theorem 3 (rank- r) is quite pessimistic compared to the known-to-be-optimal prediction of Theorem 5 (correlation).

- Except for the case $p = r = 2$ (see discussion below), the choice of p has no noticeable effect on the correlation performance, even when the (local) optimum found is not rank-deficient.
- Other properties change markedly from one graph to another.
 - **Noise tolerance:** The performance phase transition occurs soonest (i.e., for the smallest σ) for the large, sparse, and structured SLAM graph (Figure 4). The highly structured circulant graph (Figure 2) is next. The Erdős–Rényi graph (Figure 3) can tolerate the most noise.
 - **Runtime:** The runtimes follow the same trend as noise tolerance. The Erdős–Rényi graph (Figure 3) has by far the shortest runtimes. The circulant graph (Figure 2) has runtimes more than an order of magnitude higher, despite having the same size and (approximately) the same number of edges. The larger and sparser SLAM graph (Figure 4) has by far the largest runtimes.
 - **Solution rank:** For the circulant graph (Figure 2), the solution rank is almost never larger than 8 even at very high noise levels. This is likely due to the simple graph structure. For the other graphs, the solution rank increases steadily for σ near and above the phase transition.
 - **Local optima for small p :** For the case $p = r = 2$ (which, in our experiments, is SO(2) or angular synchronization), the Erdős–Rényi graph shows no problem with bad local optima for lower noise levels (curiously, the correlation performance is *higher* than for larger p). This agrees with the Kuramoto oscillator results on Erdős–Rényi graphs such as [13]. On the other hand, the algorithm is clearly finding bad local optima for the other, more structured graphs. Choosing $p = 3$ is adequate for the most part, though for the SLAM graph (Figure 4), the algorithm also occasionally stops in a full-rank local optimum (but without any apparent loss of correlation performance).

Acknowledgments

We thank Pedro Abdalla, Afonso Bandeira, Johan Markdahl, David Rosen, and Alex Townsend for helpful conversations.

References

- [1] L. Carlone, R. Tron, K. Daniilidis, and F. Dellaert, “Initialization techniques for 3d SLAM: A survey on rotation estimation and its use in pose graph optimization,” in *Proc. IEEE Conf. Robot. Autom. (ICRA)*, (Seattle, Washington, USA), May 2015.
- [2] L. Wang, A. Singer, and Z. Wen, “Orientation determination of cryo-EM images using least unsquared deviations,” *SIAM Journal on Imaging Sciences*, vol. 6, pp. 2450–2483, Jan. 2013.
- [3] D. Martinec and T. Pajdla, “Robust rotation and translation estimation in multiview reconstruction,” in *Proc. Conf. Comput. Vis. Pattern Recog. (CVPR)*, (Minneapolis, Minnesota, USA), June 2007.
- [4] M. A. Iwen, B. Preskitt, R. Saab, and A. Viswanathan, “Phase retrieval from local measurements: Improved robustness via eigenvector-based angular synchronization,” *Appl. Comput. Harmon. Anal.*, vol. 48, pp. 415–444, 2020.

- [5] J. Markdahl, J. Thunberg, and J. Goncalves, “High-dimensional Kuramoto models on Stiefel manifolds synchronize complex networks almost globally,” *Automatica*, vol. 113, 2020.
- [6] I. Waldspurger and A. Waters, “Rank optimality for the Burer–Monteiro factorization,” *SIAM J. Optim.*, vol. 30, no. 3, pp. 2577–2602, 2020.
- [7] N. Boumal, V. Voroninski, and A. S. Bandeira, “Deterministic guarantees for Burer-Monteiro factorizations of smooth semidefinite programs,” *Commun. Pure Appl. Math.*, vol. 73, no. 3, pp. 581–608, 2019.
- [8] L. O’Carroll, V. Srinivas, and A. Vijayaraghavan, “The Burer-Monteiro SDP method can fail even above the Barvinok-Pataki bound,” in *Proc. Conf. Neural Inf. Process. Syst. (NeurIPS)*, (New Orleans, Louisiana), pp. 31254–31264, Dec. 2022.
- [9] A. S. Bandeira, N. Boumal, and V. Voroninski, “On the low-rank approach for semidefinite programs arising in synchronization and community detection,” in *Proc. Conf. Learn. Theory (COLT)*, (New York), June 2016.
- [10] S. Ling, “Solving orthogonal group synchronization via convex and low-rank optimization: Tightness and landscape analysis,” *Math. Program.*, 2022.
- [11] D. M. Rosen, L. Carlone, A. S. Bandeira, and J. J. Leonard, “SE-sync: A certifiably correct algorithm for synchronization over the special Euclidean group,” *Int. J. Robot. Res.*, vol. 38, no. 2-3, pp. 95–125, 2019.
- [12] F. Dellaert, D. M. Rosen, J. Wu, R. Mahony, and L. Carlone, “Shonan rotation averaging: Global optimality by surfing $SO(p)^n$,” in *Proc. European Conf. Comput. Vis. (ECCV)*, (Virtual conference), pp. 292–308, Aug. 2020.
- [13] P. Abdalla, A. S. Bandeira, M. Kassabov, V. Souza, S. H. Strogatz, and A. Townsend, “Expander graphs are globally synchronising,” Oct. 2022.
- [14] A. S. Bandeira and R. van Handel, “Sharp nonasymptotic bounds on the norm of random matrices with independent entries,” *Ann. Probab.*, vol. 44, no. 4, pp. 2479–2506, 2016.
- [15] J. Markdahl, J. Thunberg, and J. Goncalves, “Towards almost global synchronization on the Stiefel manifold,” in *Proc. IEEE Conf. Decision Control (CDC)*, (Miami, Florida, USA), Dec. 2018.
- [16] N. Boumal, *An Introduction to Optimization on Smooth Manifolds*. Cambridge University Press, 2023.
- [17] A. Townsend, M. Stillman, and S. H. Strogatz, “Dense networks that do not synchronize and sparse ones that do,” *Chaos*, vol. 30, no. 8, 2020.
- [18] J. Markdahl, J. Thunberg, and J. Goncalves, “Almost global consensus on the n -sphere,” *IEEE Trans. Autom. Control*, vol. 63, no. 6, pp. 1664–1675, 2018.
- [19] J. Markdahl, D. Proverbio, L. Mi, and J. Goncalves, “Almost global convergence to practical synchronization in the generalized Kuramoto model on networks over the n -sphere,” *Commun. Phys.*, vol. 4, 2021.
- [20] A. Hatcher, *Algebraic Topology*. Cambridge University Press, 2001.
- [21] J. Markdahl, “Synchronization on Riemannian manifolds: Multiply connected implies multi-stable,” *IEEE Trans. Autom. Control*, vol. 66, no. 9, pp. 4311–4318, 2021.

- [22] B. Geshkovski, C. Letrouit, Y. Polyanskiy, and P. Rigollet, “A mathematical perspective on transformers,” 2023.
- [23] S. Lojasiewicz, “Sur les trajectoires du gradient d’une fonction analytique,” in *Seminari di Geometria, Università di Bologna*, pp. 115–117, Dec. 1983.
- [24] C. Lageman, *Convergence of gradient-like dynamical systems and optimization algorithms*. PhD thesis, Universität Würzburg, 2007.
- [25] M. A. Lohe, “Non-Abelian Kuramoto models and synchronization,” *J. Phys. A*, vol. 42, no. 39, p. 395101, 2009.
- [26] K. J. Doherty, D. M. Rosen, and J. J. Leonard, “Performance guarantees for spectral initialization in rotation averaging and pose-graph SLAM,” in *Proc. IEEE Conf. Robot. Autom. (ICRA)*, (Philadelphia, PA, USA), May 2022.
- [27] A. Y. Zhang, “Exact minimax optimality of spectral methods in phase synchronization and orthogonal group synchronization,” Sept. 2022.
- [28] R. Hartley, J. Trumpf, Y. Dai, and H. Li, “Rotation averaging,” *Int. J. Comput. Vis.*, vol. 103, pp. 267–305, 2013.
- [29] D. M. Rosen, K. J. Doherty, A. T. Espinoza, and J. J. Leonard, “Advances in inference and representation for simultaneous localization and mapping,” *Annual Review of Control, Robotics, and Autonomous Systems*, vol. 4, pp. 215–242, May 2021.
- [30] S. Burer, R. D. C. Monteiro, and Y. Zhang, “Rank-two relaxation heuristics for MAX-CUT and other binary quadratic programs,” *SIAM J. Optim.*, vol. 12, no. 2, pp. 503–521, 2002.
- [31] S. Burer and R. D. C. Monteiro, “Local minima and convergence in low-rank semidefinite programming,” *Math. Program.*, vol. 103, pp. 427–444, 2005.
- [32] N. Boumal, “A Riemannian low-rank method for optimization over semidefinite matrices with block-diagonal constraints,” tech. rep., 2015.
- [33] S. Mei, T. Misiakiewicz, A. Montanari, and R. I. Oliveira, “Solving SDPs for synchronization and MaxCut problems via the Grothendieck inequality,” in *Proc. Conf. Learn. Theory (COLT)*, (Amsterdam, Netherlands), July 2017.
- [34] R. Y. Zhang, “Improved global guarantees for the nonconvex burer–monteiro factorization via rank overparameterization,” 2022.
- [35] A. Singer and H. tieng Wu, “Vector diffusion maps and the connection Laplacian,” *Commun. Pure Appl. Math.*, vol. 65, no. 8, pp. 1067–1144, 2012.
- [36] A. Singer, “Angular synchronization by eigenvectors and semidefinite programming,” *Appl. Comput. Harmon. Anal.*, vol. 30, pp. 20–36, 2011.
- [37] A. S. Bandeira, A. Singer, and D. A. Spielman, “A Cheeger inequality for the graph connection Laplacian,” *SIAM J. Matrix Anal. Appl.*, vol. 34, no. 4, pp. 1611–1630, 2013.
- [38] A. S. Bandeira, “Random Laplacian matrices and convex relaxations,” *Found. Comput. Math.*, vol. 18, pp. 345–379, 2018.
- [39] L. Wang and A. Singer, “Exact and stable recovery of rotations for robust synchronization,” *Inform. Inference.*, vol. 2, no. 2, pp. 145–193, 2013.

- [40] F. Filbir, F. Kraemer, and O. Melnyk, “On recovery guarantees for angular synchronization,” *J. Fourier Anal. Appl.*, vol. 27, 2021.
- [41] B. P. Preskitt, “Phase retrieval from locally supported measurements,” 2018.
- [42] C. Gao and A. Y. Zhang, “Exact minimax estimation for phase synchronization,” *IEEE Trans. Inf. Theory*, vol. 67, no. 12, pp. 8236–8247, 2021.
- [43] C. Gao and A. Y. Zhang, “SDP achieves exact minimax optimality in phase synchronization,” *IEEE Transactions on Information Theory*, vol. 68, pp. 5374–5390, Aug. 2022.
- [44] S.-Y. Ha, D. Ko, J. Park, and X. Zhang, “Collective synchronization of classical and quantum oscillators,” *EMS Surveys in Mathematical Sciences*, vol. 3, no. 2, pp. 209–267, 2016.
- [45] A. Pikovsky and M. Rosenblum, “Introduction to focus issue: Dynamics of oscillator populations,” *Chaos*, vol. 33, no. 1, 2023.
- [46] R. Taylor, “There is no non-zero stable fixed point for dense networks in the homogeneous Kuramoto model,” *J. Phys. A*, vol. 45, 2012.
- [47] S. Ling, R. Xu, and A. S. Bandeira, “On the landscape of synchronization networks: A perspective from nonconvex optimization,” *SIAM J. Optim.*, vol. 29, no. 3, pp. 1879–1907, 2019.
- [48] R. Yoneda, T. Tatsukawa, and J. nosuke Teramae, “The lower bound of the network connectivity guaranteeing in-phase synchronization,” *Chaos*, vol. 31, no. 6, 2021.
- [49] J. Lu and S. Steinerberger, “Synchronization of Kuramoto oscillators in dense networks,” *Nonlinearity*, vol. 33, no. 11, pp. 5905–5918, 2020.
- [50] M. Kassabov, S. H. Strogatz, and A. Townsend, “Sufficiently dense Kuramoto networks are globally synchronizing,” *Chaos*, vol. 31, no. 7, 2021.
- [51] M. Kassabov, S. H. Strogatz, and A. Townsend, “A global synchronization theorem for oscillators on a random graph,” Mar. 2022.
- [52] P. Abdalla, A. S. Bandeira, and C. Invernizzi, “Guarantees for spontaneous synchronization on random geometric graphs,” Aug. 2022.
- [53] J. Markdahl, “A geometric obstruction to almost global synchronization on riemannian manifolds,” Aug. 2018.
- [54] L. DeVille, “Synchronization and stability for quantum Kuramoto,” *J. Stat. Phys.*, vol. 174, pp. 160–187, 2019.
- [55] M. Journée, F. Bach, P.-A. Absil, and R. Sepulchre, “Low-rank optimization on the cone of positive semidefinite matrices,” *SIAM J. Optim.*, vol. 20, no. 5, pp. 2327–2351, 2010.
- [56] R. A. Horn and C. R. Johnson, *Topics in Matrix Analysis*. Cambridge University Press, 1991.
- [57] A. E. Rastegin, “Relations for certain symmetric norms and anti-norms before and after partial trace,” *J. Stat. Phys.*, vol. 148, pp. 1040–1053, Aug. 2012.
- [58] T. Pumar, S. Jelassi, and N. Boumal, “Smoothed analysis of the low-rank approach for smooth semidefinite programs,” in *Proc. Conf. Neural Inf. Process. Syst. (NeurIPS)*, (Montréal, Canada), pp. 2281–2290, Dec. 2018.
- [59] N. Boumal, B. Mishra, P.-A. Absil, and R. Sepulchre, “Manopt, a Matlab toolbox for optimization on manifolds,” *J. Mach. Learn. Res.*, vol. 15, no. 42, pp. 1455–1459, 2014.